DEPENDENCE OF THE ENTHALPY AND VAPOR PRESSURE OF KRAFT BLACK LIQUOR ON SOLIDS CONTENT

By

MARK A. STOY

A DISSERTATION PRESENTED TO THE GRADUATE SCHOOL
OF THE UNIVERSITY OF FLORIDA IN PARTIAL FULFILLMENT
OF THE REQUIREMENTS FOR THE DEGREE OF
DOCTOR OF PHILOSOPHY

UNIVERSITY OF FLORIDA
1992

UNIVERSITY OF FLORIDA LIBRARIES

TABLE OF CONTENTS

LIST OF TABLES iv

LIST OF FIGURES v

ABSTRACT vii

INTRODUCTION AND OVERVIEW 1

BACKGROUND 5

- Description of Kraft Black Liquor 5
- Previous Work 9

MATERIALS AND METHODS 13

- Liquor Selection 13
- Solution Calorimetry 15
- Differential Scanning Calorimetry 20
- Vapor-Liquid Equilibrium 24

PRESENTATION AND ANALYSIS OF RESULTS 27

- Data Presentation 27
  - Enthalpy-Concentration Charts 27
  - Heat of Dilution Results 28
  - Heat Capacity Results 34
  - Vapor Pressure Results 39
  - Calculated Vapor Pressures 42
- Data Analysis 44

CONCLUSIONS AND RECOMMENDATIONS 51

APPENDIX A DETAILED DISCUSSION OF THE ENTHALPY WORK . 54

- Derivation of the Working Equation for the Enthalpy Scale 54
- Construction of the Chart 56
- Enthalpy Tables 57
- Heat Capacity Measurements 61
  - Importance of the Standard Run with Sapphire 61
  - Stainless Steel Pans 62
  - Sample Size 64

Method of Data Analysis 65
Uncertainty Analysis 67

APPENDIX B DETAILED DISCUSSION OF THE VAPOR PRESSURE WORK 72

Relationship Between the Enthalpy and Vapor Pressure 72
Calculation of Vapor Pressures from Enthalpy Data 74

REFERENCE LIST 76

BIOGRAPHICAL SKETCH 78

LIST OF TABLES

Table Page

1 Typical composition of organic material in pine Kraft black liquor 7

2 Typical property values at different stages of concentration 8

3 Pulping conditions for experimental liquors 14

4 Kappi numbers for experimental liquors 14

5 Comparison of calculated and experimental vapor pressures for L51 43

6 Comparison of BPE estimates with literature values 50

7 Enthalpy for liquor L1 58

8 Enthalpy for liquor L31 59

9 Enthalpy for liquor L51 60

10 Heat capacity results for three samples of the same solids content 70

11 Mean and standard deviation of samples for uncertainty analysis 71

LIST OF FIGURES

Figure Page

1 Heat capacity behavior at high solids contents. 10

2 Mixing cell used for dilution experiments 17

3 Power response curve for a dilution experiment 19

4 Schematic of the measuring head for a power compensated DSC 21

5 DSC scans used to determine the heat capacity of a sample 23

6 Schematic of vapor pressure apparatus 25

7 Enthalpy-concentration chart for liquor L1 29

8 Enthalpy-concentration chart for liquor L23 29

9 Enthalpy-concentration chart for Liquor L31 30

10 Enthalpy-concentration chart for liquor L51 30

11 Plot of the total heat of dilution for a series of dilutions 31

12 Heat absorbed to dilute black liquor to infinite dilution 33

13 Base isotherm and definition of infinite dilution reference state 33

14 Heat capacity vs. temperature data for Liquor L1 36

15 Heat capacity vs. temperature data for liquor L23 36

16 Heat capacity vs. temperature data for liquor L31 37

17 Heat capacity vs. temperature data for liquor L51 37

18 Heat capacity vs. solids content data for liquor L51 38

19 Vapor pressure versus temperature at three solids contents for liquor L51 40

20 Vapor pressure versus temperature behavior at 30% solids 40

21 Vapor pressure versus temperature behavior at 50% solids 41
22 Vapor pressure versus temperature behavior at 70% solids 41
23 Comparison of base isotherms 45
24 Fitted values of the heat capacity for liquor L1 47
25 Fitted values of the heat capacity for liquor L51 47
26 Boiling point elevation plot for liquor L51 48
27 Comparison of calculated and measured vapor pressures for liquor L51 .. 50
28 Method for aligning ending isotherms. 66
29 Sample calculation for uncertainty in Cp measurement by DSC 69

Abstract of Dissertation Presented to the Graduate School
of the University of Florida in Partial Fulfillment of the
Requirements for the Degree of Doctor of Philosophy

DEPENDENCE OF THE ENTHALPY AND VAPOR PRESSURE OF KRAFT BLACK LIQUOR ON SOLIDS CONTENT

By

Mark A. Stoy

May, 1992

Chairperson: A. L. Fricke
Major Department: Chemical Engineering

Data for the equilibrium properties of kraft black liquor were developed for four different liquors from laboratory cooks of slash pine. The enthalpy change for concentrating black liquor over the range of 0-80% solids and 40-120 °C can now be determined easily from enthalpy concentration charts. The charts incorporate, for the first time, the heat of solution effect for separating water from black liquor into the energy balance around the evaporators. Vapor pressure data, consistent with the enthalpy charts, were developed for the same set of liquors.

Since the charts are useful for binary mixtures only, black liquor was assumed to be a pseudo-binary mixture of pure solids and water. One isotherm of the charts was determined from heats of dilution which were measured at 80 °C by solution calorimetry. Samples of black liquor were diluted from 80% solids down to a low solids content in a series of dilutions. The total heat evolved to dilute black liquor from a given solids content to infinite dilution was determined from these data. The remaining isotherms were determined from heat capacity data which were measured by differential scanning calorimetry.

The vapor pressure of water over black liquor was measured as a function of solids content and pressure by using an equilibrium still. From these results, the boiling point elevation was determined as a function of solids content and pressure.

The difference among the enthalpy charts for the four liquors studied was negligible. This suggests that all black liquors are the same in terms of the enthalpy and that they can be treated as a binary mixture of solids and water. There was no significant difference in the heats of dilution for any of the liquors. The heat capacity was found to change non-linearly with increasing solids content above 30% solids. This behavior, however, was not observed for all the liquors studied. The boiling point elevation was similar for all the liquors studied and was in the range of values in the literature.

INTRODUCTION AND OVERVIEW

The Kraft recovery cycle recovers the inorganic chemicals from black liquor and disposes of the organic by-products from pulping. It is a large complex process, which is necessary for Kraft pulping to be economically feasible. Kraft recovery operations in the U.S. and Canada process about 80 x 10^6 tons of black liquor solids annually. The industrial significance of this capital and energy intensive process is generally not recognized outside of the paper industry.

The organic by-products from pulping are disposed of by burning them in the Kraft recovery boiler. The resulting energy of combustion is used to produce to high pressure steam for power generation. The spent cooking chemicals are partially regenerated in the boiler and are then recovered for further processing. The operation of the recovery cycle and the mill depend upon the recovery boiler performing these two functions.

Although the Kraft recovery boiler serves its purpose well, the thermal efficiency of the boiler is low. A large amount of the energy released in the boiler is not recovered because it is used to evaporate the remaining water in the firing liquor. If the liquor was concentrated to higher solids contents in the evaporators, more energy could be recovered for power generation. The resulting energy savings of a more concentrated firing liquor is large because the evaporators remove water more efficiently than the recovery boiler. The evaporators operate at a 4-to-1 steam economy, which means that 4 pounds of water are evaporated for every pound of steam consumed. In contrast, the steam economy of the recovery boiler is about 1-to-1.

A more concentrated firing liquor would reduce the amount of water evaporated in the furnace, increase the capacity of the furnace, and improve safety. Prior to 1980, when energy prices were low, there was little economic incentive to improve the thermal efficiency of the recovery cycle. The design of the recovery boiler had matured without a clear understanding of the combustion processes and chemical reactions that take place inside it. To increase the solids limit of the firing liquor would have required a large expensive R & D program beyond the resources of a single paper company.

When energy prices rose in the early 1980s, the U.S. Department of Energy began funding and coordinating research to advance black liquor recovery technology. The goal of this program was to increase the solids content limit from the present 65% to 75% or above. Naturally, many programs were started to develop a fundamental understanding of the processes occurring inside the furnace. It was also recognized that without improved data for the physical properties of black liquor future development of recovery technology would be hampered. As a result, a comprehensive program was started in 1982 to measure the physical properties of Kraft black liquor. This program is now in the Department of Chemical Engineering at the University of Florida.

The black liquor physical property program is designed to determine how the pulping conditions and composition affect the rheological and equilibrium properties of black liquor. A series of well characterized liquors, pulped under carefully controlled conditions, are being used for this work. The rheological properties are the most important properties to understand for processing black liquor. They affect a number of different processes from heat transfer in the evaporators to droplet formation and combustion in the furnace.

Accurate enthalpy and vapor pressure data are necessary to size and operate the evaporators for black liquor concentration. Although there are data for the vapor pressure, there are no complete enthalpy data for black liquor. The only enthalpic data available now are heat capacities. As a result, the evaporators are designed with an approximate energy balance that ignores the enthalpy change for separating water from black liquor. Our present knowledge of the available data for the heat capacity and vapor pressure is incomplete. Past research has not established how much these properties vary from liquor to liquor or how much they change with solids contents above 60%. Previous studies have assumed that black liquor is a mixture of solids and water. But, it has not been determined if black liquor needs to be characterized beyond the concept of a mixture of solids and water. Thus, we do not whether the difference in the reported results is due to compositional differences between liquors or due to experimental error.

The data for the vapor pressure and enthalpy of black liquor should be developed in a manner to similar to that of other commercially important systems. Complete enthalpy data should be measured and then used to develop a database for the enthalpy and vapor pressure that is thermodynamically consistent. An enthalpy concentration chart is a convenient way to represent enthalpy data. It gives the change in enthalpy as function of composition and temperature. These charts have been developed for many other applications. A similar chart should be developed for black liquor. The enthalpy data can then be used to check the vapor pressure data for consistency by using a standard thermodynamic treatment.

Consequently, the purpose of this research was to develop a consistent set of enthalpy and vapor pressure data for black liquor. We were interested in answering the following two questions:

1. How do the enthalpy and vapor pressure change with increasing solids content? In particular, how do they change above 60% solids?
2. How much do the enthalpy and vapor pressure change from liquor to liquor when compared at the same solids content?

We chose a series of well characterized laboratory liquors covering a wide range of pulping conditions to begin this work. Enthalpy data were derived from measurements of the heat capacity and heat of dilution. The vapor pressure of water over black liquor was measured for the same set of liquors.

This dissertation presents the results of my research on the enthalpy and vapor pressure properties of black liquor. In the remaining sections, I first give a description of black liquor and then describe the previous work for the enthalpy and vapor pressure. Then, the three types of experiments that were used are discussed. Finally, the results are given and discussed. The appendices give a more detailed discussion of the experiments and data analysis for those readers who want more information on these subjects.

BACKGROUND

Description of Kraft Black Liquor

The Kraft pulping process is used almost exclusively because of its versatility with a wide range of raw materials, its high pulp strength, and the well-established methods for processing the spent cooking liquor. In Kraft pulping, wood chips are reacted with a strong alkaline solution of sodium hydroxide and sodium sulfide at elevated temperatures. The cooking liquor acquires a deep brown color during pulping, hence its name, black liquor. Once the liquor is separated from the pulp, it becomes a waste stream which cannot be discharged to the environment.

The liquor that is sent to the recovery cycle for disposal is a dilute solution of 10-15% solids. It is first concentrated to about 65% solids by multiple-effect evaporation. As the liquor is concentrated, it becomes more and more viscous because of its high organic content. The concentrated liquor is then burned in the recovery boiler to dispose of the organics. The inorganics fall to the bottom of the furnace where the sulfur ions are reduced in the char bed to form sodium sufide. A smelt of molten sodium salts is withdrawn from the boiler, dissolved in water, reacted with lime, and then clarified. The clarified solution is recycled back to the pulping process.

On a dry solids basis, the organics make up about 50% to 65% of the total solids in black liquor; The remaining solids are inorganics from the spent cooking chemicals. The composition of the solids is controlled by the pulping conditions and wood species. The major components of the solids can be grouped into classes as sodium salts, lignin, C1 to C5 organic acids, and hydroxy acids. The reactions between the cooking chemicals and wood components, however, create many more components in trace amounts. The principal sodium salts are sodium carbonate, sodium sulfate, and sodium sulfide.

There are two major components that make up the organics in black liquor solids. Lignin constitutes about half of the total organic content. The other major component of the organics is the hydroxy acids of which there are many (see Table 1). These acids are formed from reactions with the carbohydrates, particularly the hemicellulose, in the wood. Hardwoods and softwoods contain different types and amounts of lignin and hemicellulose. Thus, the relative composition of the organics will also be affected by the pulping conditions and wood species. Although Table 1 does not show all the organic components, it suggests how complex the composition of black liquor is.

The lignin molecule consists of a large number of polymerized phenyl-propane units containing carboxylic, ether, and hydroxyl groups. Its exact structure, however, is unknown. In wood, lignin is a three-dimensional network polymer that gives wood its rigidity and holds the cellulose fibers in place. This network structure is attacked during pulping and broken down. In black liquor, therefore, lignin has a broad molecular weight distribution. Typical weight average molecular weights and number average molecular weights are in the range of 10,000 to 40,000 and 2,000 to 7,000, respectively.

From a processing standpoint, it is important to know how the properties of black liquor change with the solids content. Table 2 shows how the boiling point rise (BPR), viscosity, and heat capacity change as the solids content increases. The viscosity of the liquor may change by as much as two orders of magnitude. Note that the viscosity begins to increase more rapidly around 50% solids. In this region, there is a transition from a water continuous phase to an organic continuous phase. The heat

Table 1. Typical composition of organic material in pine Kraft black liquor. Source: Table taken from Sjostrom, 1981.

Component	Content (% of dry solids)	Composition (% of hydroxy acids)
Lignin	47	
Hydroxy acids	28	
Lactic		15
2-Hydroxybutanoic		5
2,5-Dihydroxypentanoic		4
Xyloisosaccharinic		5
α-Glucoisosaccharinic		15
β-Glucoisosaccharinic		36
Others		20
Formic acid	7	
Acetic acid	4	
Extractives	5	
Other compounds	9	

capacity changes as one would expect it to; It starts at a value of one for pure water and decreases as the solids content increases.

Although the amount of solids is a convenient composition variable for the properties of black liquor, it simplifies black liquor to a mixture of solids and water. The properties of black liquor, however, depend upon the composition of the solids. Thus, a given property will have different values when compared at the same solids content for different liquors. Some properties may depend only on the overall

Table 2. Typical property values at different stages of concentration. Source: Data taken from Adams and Frederick, 1988.

	Solids %	Temp. °F	BPR °F	Viscosity cps	Cp Btu/lb-F
weak liquor	15	170	2.5	0.7	0.93
liquor in evaps	21	165	3.5	0.9	0.90
liquor in evaps	35	270	7.5	0.8	0.85
liquor in evaps	50	220	14.5	5.0	0.77
liquor in evaps	65	220	25.0	63.0	0.71
high solids liquor	80	295	48.0	253	0.64

composition of the solids, such as the amount of inorganics, for example, and other properties may depend on the relative composition of the organics. Properties that depend on the overall composition will not change much because the overall composition of black liquor does not change significantly from liquor to liquor. The composition of the organics and molecular weight distribution of lignin are more sensitive to the pulping conditions and wood species. Properties that depend on the relative composition of the organics, such as the viscosity, can be expected to vary significantly among different liquors. In addition, these properties may also depend on the molecular weight distribution of lignin.

Previous Work

Harvin and Brown (1953) measured the heat capacity of a mill liquor, pulped from southern pine, over the range of 100-200 °F and 5-53% solids contents. They found that the heat capacity increased linearly with increasing temperature and decreased linearly with decreasing solids content. Harvin and Brown developed the empirical equation,

$$Cp = 0.990 + 8.0 x 10^{-5} T - (0.639 - 6.4 x 10^{-4} T) C$$

where T is the temperature in degrees fahrenheit and C is the weight fraction of solids, to represent their data. Earlier data had showed no correlation with temperature. On this basis, they showed that their results differed significantly over the earlier data for the operating conditions of the evaporators. These data have been widely used for energy balances and design of evaporators since.

Masse (1984,1987) published the next complete set of heat capacity data for two black liquors from laboratory cooks of southern pine. He measured the heat capacity using differential scanning calorimetry over the range of 65-105 °C and 0-99% solids contents. Masse found that the heat capacity did not vary linearly with increasing solids content above 30% solids. The heat capacity above 30% solids was higher than what a straight line extrapolation of the low solids data would predict (see Figure 1). This deviation was about 6% higher at its maximum. Masse was able to fit his data to

$$Cp = Cp_1 w_1 + Cp_2 w_2 + \gamma w_1 w_2^m$$

where Cp is the heat capacity of the mixture, Cp_i is the heat capacity of component *i*, w_i is the mass fraction of component *i*, γ is a temperature-dependent parameter, and m a temperature-independent parameter. The first two terms represent the heat capacity

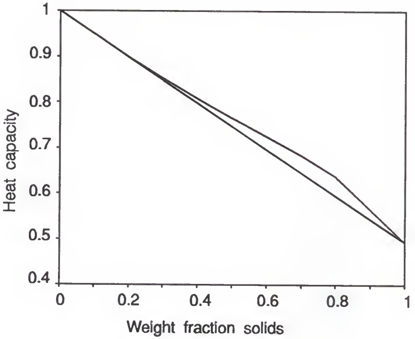

Figure 1. Heat capacity behavior at high solids contents. Source: Data obtained from Masse, 1984.

of an ideal mixture of pure black liquor solids and water. The last term, borrowed from the lattice theory of polymer solutions, was used to account for the deviation from an ideal mixture. For ideal behavior, this term would be zero and the heat capacity would be a straight line extending from 1.0 for pure water to a value for pure solids.

The values of the heat capacity predicted by the above equation do not change much with temperature. Starting at 60% solids, the values actually decrease with increasing temperature. This behavior was not discussed by Masse and is in contrast to the data reported by Harvin and Brown.

Complete enthalpy data are developed from heats of solution and heat capacities. The heat of solution for mixing black liquor with water has not been measured and, as a result, there are no complete enthalpy data available for black liquor today. Jelinek (1986), however, tried to develop enthalpy tables for black liquor using the heat capacity data of Harvin and Brown. Unfortunately, Jelinek's approach is flawed since it is not possible to generate enthalpy data from heat capacity data alone.

Jelinek added a simple expression for the heat of mixing of black liquor solids with water to the enthalpy of an ideal mixture of black liquor solids and water. This term is analogous to the term used by Masse for the excess heat capacity. The heat of mixing term contained a single constant and correctly allowed for the heat of mixing to go to zero for pure water or pure solids. When the resulting expression for the enthalpy was rearranged, it could be fitted to enthalpy data to obtain the equation's two constants, the heat of mixing constant, and the enthalpy of pure solids. The enthalpy data were obtained by integrating heat capacity data for black liquor and water. Jelinek's mistake was to assume a reference temperature for the mixture instead of specifying reference states for the pure components. This allowed him to integrate the heat capacity data from a reference temperature where he specified the enthalpy to be zero. When I plotted the resulting enthalpy data versus solids content, I found the isotherms to be straight lines showing that the enthalpy of mixing is zero. Jelinek's analysis, as a result, is nothing more than data fitting.

There have been a number of studies of the vapor pressure of water over black liquor (see Fricke, (1987), for a list of them). The vapor pressure is usually measured with an equilibrium still or by slow evaporation from an evaporator, which is not a true equilibrium measurement. Some of the reported work has been taken from commercial plant evaporators.

The vapor pressure of black liquor is difficult to measure because of the superheating that occurs in the liquor as the solids content increases. This makes it difficult to record the true boiling point of the liquor. The results are usually expressed in terms of the boiling point elevation (BPE), which is the difference between the boiling point of the solution and pure water at the same pressure. The available data show that the BPE increases rapidly in an exponential type relationship with increasing solids content.

The most complete set of vapor pressure data, 0-90% solids, were reported by Szymonski and Grace (1985) using an isopiestic technique. Black liquor solutions were equilibrated through the vapor phase with salt solutions of known vapor pressure. The final moisture content of the black liquor samples was determined from the difference between the initial and final sample weights. With this technique, they could eliminate the superheating that occurs in a typical equilibrium still. Their apparatus, however, was crude compared to the types that had been reported in the literature for electrolytes and their temperature control was also poor. They reported BPE values of 4 °C and 17 °C at 25% and 65% solids contents, respectively. Their results follow the trend of other BPE data for black liquor but are offset to higher values. They also took enough data to determine the effect of pressure on the BPE, but they did not extract this information.

Clay and Grace (1984) measured the BPE using an equilibrium still. They recognized the problem of superheating and, as a result, used an oil to disperse the black liquor. They measured the BPE of black liquor and oil mixtures from 45% to 85% solids. They also measured the BPE for pure black liquor (oil free) below 65% solids. This technique, however, was not successful below 65% solids because the oil/black liquor data showed a larger BPE than the pure black liquor data. Above 75% solids, the superheating for the oil/black liquor data was much smaller. They combined their oil-free data below 65%, the oil/black liquor data, and other data to obtain a best-fit estimate of the BPE from 40% to 90% solids. Their data are about 5 degrees lower than the data reported by Szymonski and Grace.

MATERIALS AND METHODS

Liquor Selection

Because black liquor is a highly variable material, the liquors must be chosen carefully to ensure that the results are meaningful. In a study comparing the properties of different liquors to determine what variables control them, the source and handling of the liquors should be carefully controlled. Usually this is not possible with liquors obtained from a mill. If the liquors are produced from laboratory cooks, then tight control can be maintained over the pulping and handling of the liquors. Laboratory liquors, however, may not be the same as mill liquors in terms of the behavior of some of the properties.

This research is part of a larger, more comprehensive research program funded by the Department of Energy to develop a database for the physical properties of black liquor (Fricke, 1983). The success of this program depends on having a set of well-defined liquors. For this reason, laboratory liquors are carefully produced from a statistically designed pulping experiment. The pulping experiment, which covers a wide range of pulping conditions, controls four pulping variables (Fricke, 1983). The four variables are the cooking time, temperature, effective alkali, and sulfidity. The Kappa numbers for these conditions range from 25 to 90. The statistical experiment permits properties to be related to the pulping conditions. The effect of each variable as well as the interaction between variables can be determined. Later, mill liquors will be incorporated into the overall program to increase the reliability of the database.

Table 3. Pulping conditions for experimental liquors

Liquor	Time Minutes	Temperature °F	Effective Alkali %	Sulfidity %
L1	60	340	14.5	12.5
L5	60	340	14.5	42.5
L7	100	340	14.5	27.5
L23	40	330	13.0	20.0
L31	80	330	16.0	20.0
L51	80	350	16.0	35.0

Table 4. Kappi numbers for experimental liquors

Liquor	Kappa No.
L1	25.8
L5	36.5
L7	25.4
L23	106.8
L31	61.1
L51	18.5

Since this is the first attempt at measuring heats of solution for black liquor, the laboratory liquors from the pulping experiment were used. The pulping was done at the University of Florida in our own pilot plant using slash pine as the wood source (Fricke, 1989). Briefly, we have a small batch digester for pulping, a wiped-film evaporator for concentration, and associated tankage for chemical make up and storage. The digester, a 26.5 gallon pressurized vessel, is 1/1000 to 1/2000 the size of a commercial digester. It is heated by steam and can be operated either as a tumbling autoclave or as a stationary reactor with a pump for circulating the liquor during cooking.

The pulping conditions for the liquors used in this work are shown in Table 3. The liquors were chosen so that a wide range of behavior might be expected. Liquors L23 and L51 are from the extreme points of the pulping experiment. Liquor L23 represents the mildest conditions and L51 the harshest conditions. The Kappa numbers for the liquors are given in Table 4. Each liquor is a combination of two liquors that were made from two identical pulping runs. The liquors were combined only when the Kappa numbers agreed within 10 percent. The values in Table 4, therefore, are the averages for two pulping experiments.

Solution Calorimetry

Samples of black liquor were diluted with water and the resulting heats of dilution measured by solution calorimetry. Each liquor was diluted in a series of steps starting from a sample of 80% solids down to a solution of low solids content. The purpose of these measurements was to determine the total heat of dilution. From the total heat of dilution, one isotherm of the enthalpy concentration chart was determined.

The heats of dilution were measured with a Setaram model C-80 calorimeter, which was purchased for this work. Like other heat conduction devices, the C-80 has a large metal measuring block which is maintained at a constant temperature. The measuring block has two identical cell holders for the measuring cells. One holder is for the sample cell, and the second holder is for a reference cell. There are a number of thermocouples wired in series around each cell holder which measure the temperature difference between each cell and the block. The output from these thermocouples is proportional to the energy exchanged between the block and cells.

The purpose of the reference cell is to improve the measurement of the sample event being studied. It is used as a blank to cancel out all effects other than the one of interest in the sample cell. The output from its thermocouples is connected in parallel with those around the sample cell to give a differential output that is proportional only to the temperature difference between the sample and block. The output drops to zero when the sample cell and block are at the same temperature. A computer collects this power signal as a function of time. The area under the power versus time curve is proportional to the enthalpy change for the experiment.

The calorimeter is equipped with a motor driven reversing device which rotates the measuring block 180 degrees back and forth to mix the components. The calorimeter was calibrated originally by Setaram using a joule heating technique. We checked the calibration by using a calorimetry standard, the heat of mixing for KCl and water.

The principal parts of the mixing cells are shown in Figure 2. The insert holds one of the components to be mixed and screws into the bottom of the cell. It has a usable volume of about 1.35 ml. The cavity formed by the insert and body holds the other component to be mixed. The lid that separates the two components does not form a leak-tight seal with the insert. To keep the components from pre-mixing, a sealing agent is added to the annular space around the insert to cover the lid. Mercury is usually used as the sealing agent because it has a high density and surface tension.

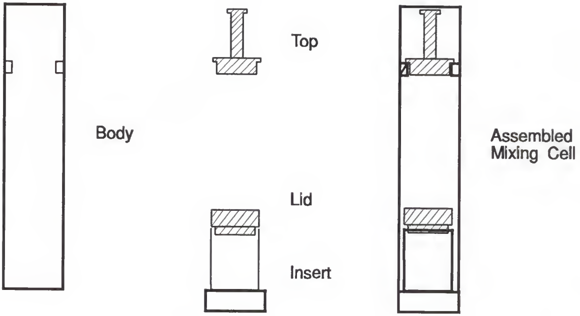

Figure 2. Mixing cell used for dilution experiments

When the minimum amount of sealing agent is used, the upper cavity has a usable volume of about 3 ml. The assembled cell is placed into the calorimeter with a handle that threads on to the top of the cell.

Because mercury can react with the sulfur compounds in black liquor, it could not be used as the sealing agent. Krytox, a fluorinated oil from DuPont, was used instead. The oil, a perfluoroalkylpolyether, is colorless, odorless, and inert to a wide range of materials. It is used as a lubricating agent and vacuum pump oil under harsh conditions. For this work, the oil is attractive because it does not react with the components in black liquor or dissolve them. Krytox has a high density, 1.88 g/cc, which meant that either of the components, black liquor or water, could be floated on top of the oil. The oil, unfortunately, has a low surface tension, which meant that it mixed intimately with the mixture during mixing. The question of whether the oil affected the results was tested by comparing the heat of mixing for KCl and water with Krytox and mercury. There was no difference in the results with mercury or Krytox.

The components were weighed into the cells using an analytical balance with a 0.1 mg precision. The sample cell was filled with black liquor and water and the reference cell with water only. The insert was filled first, with either black liquor or water depending on the solids content. When the initial concentration of solids was below 60%, the black liquor sample was placed in the insert. The insert was filled to within about 2 mm of the lid. Next, the Krytox layer was added and the amount adjusted to keep the required amount of water to within about 2 mm of the top of the cell. The desired final concentration could be controlled carefully if the liquor was loaded first because it was easy to adjust the amount of water added to the cell.

Because of the viscosity above 60% solids, the components would not mix completely if the sample was loaded into the insert. The position of the components, therefore, was reversed and the sample was placed in the upper cavity. Up to about 70% solids, the material was heated and poured directly into the upper chamber of the cell. Above 70% solids, the material was too viscous to pour into the cell and had to be molded into a plug. To make a sample plug, the material was heated and packed into a plunger, made of Teflon, with a spatula. When the material had partially cooled, it was extruded from the plunger, trimmed to the correct length, and then placed in the cell. The material trimmed from the plug was used to determine the initial solids content of the sample.

The final concentration could not be controlled with the sample on top because it was difficult to make small adjustments to the amount of sample in the cell. Thus, the first dilution had to be to about 55% so that a series of dilutions with matching initial and final concentrations could be completed. It was necessary to match the initial concentration of solids for each dilution with the final concentration of solids for the previous dilution so that the individual results could be added together. Samples for each dilution were prepared by diluting a stock sample of material.

The heats of dilution were measured at 80 °C because the viscosity above 50% solids was too high for the components to mix at lower temperatures. Each dilution below 60% solids was run twice. Above 60% each dilution was made only once because it was difficult to load the same amount of sample in the cell. The cells were equilibrated in the calorimeter until the block temperature and power signals stabilized. When an experiment was started, the isothermal baseline was recorded for two minutes before mixing the components. Then, the calorimeter's rocking motor was started to mix the components. Below 70% solids, the components mixed easily and an exothermic peak developed rapidly (see Figure 3). The cells were mixed for about 5 minutes, which was enough time for the power signal to reach a maximum and then start to decrease. The first dilution was more sluggish, however, and the cells had to be

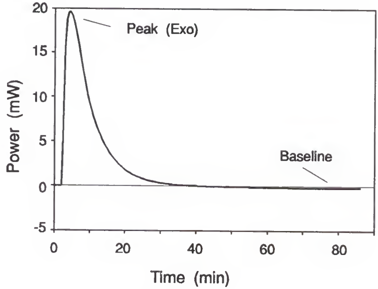

Figure 3. Power response curve for a dilution experiment

mixed for 40 to 50 minutes. When the isothermal baseline reappeared, the experiment was stopped. The area under the response curve in Figure 3 is the heat of solution. The height of the peak decreased with each dilution as solids content decreased.

Differential Scanning Calorimetry

Differential scanning calorimetry (DSC) records the flow of energy into a sample that is directly proportional to the heat capacity. From a DSC experiment, we measured the change in heat capacity with temperature for a sample of a given solids content. Samples of different solids contents were used to complete the heat capacity data over the solids range of interest. These data were used to determine the remaining isotherms for the enthalpy concentration charts.

A Series 7 DSC and computer from Perkin-Elmer were used in this work. The Series 7 DSC is completely computer controlled. Once a sample was loaded into the instrument, the parameters for the scan were selected, the scan started, and the results stored for analysis from the terminal. The operating software contains a number of graphic routines that allow one to manipulate data and perform calculations. Since it is too time consuming to calculate heat capacities for a large number of samples using the operating software, a computer program was written to perform the heat capacity calculations.

A DSC measures the differential energy needed to keep two cell holders, sample and reference, at the same temperature while changing the temperature of both cells at a controlled rate. The measuring head for a power compensated type of DSC is shown in Figure 4. The head is coupled to a heat sink, which is filled with a coolant, by a cold finger. Inside the head are the sample and reference pan holders. Each holder has its own heater and platinum resistance thermometer. The holders are kept at the same temperature by two separate control circuits. One circuit controls both heaters so that

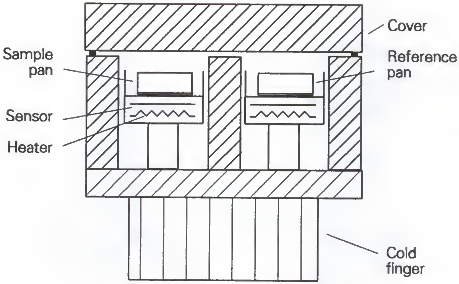

Figure 4. Schematic of the measuring head for a power compensated DSC

the average temperature of the two holders is equal to the program temperature. The second circuit compares the temperature of each holder and supplies energy to the heater of the holder, which lags the program temperature. When an endothermic transition occurs, for example, the power to the sample is increased to match the energy absorbed by the sample. For an exothermic transition, the power to the sample is reduced to allow the heat generated by the sample to flow from the cell holder to the heat sink.

The sample must be placed into a sample pan before it can be run in the DSC. Normally, aluminum pans are used for this. We had to use pans made from stainless steel instead, because black liquor corrodes aluminum. The pans, which are available from Perkin-Elmer, come in three parts: bottom, top, and O-ring. They are much larger and can withstand higher pressures than aluminum pans.

About twelve different samples were used to cover the concentration range from 15% to 80% solids. Samples were prepared by evaporation rather than trying to load the pans with concentrated samples. A pan was filled with 25% material and then allowed to evaporate to the desired final solids content before sealing it. With this procedure, I could prepare samples that were evenly distributed in the pans and had good control over the experimental error. The sample size was kept between 25 and 35 mg.

A DSC scan consisted of three parts: an isothermal hold at the initial temperature, heating to the final temperature, and an isothermal hold at the final temperature (see Figure 5). The isothermal hold at the start of each run established a zero reference point on the power axis. The initial isothermal hold was for 2 minutes at 27 ° C, and the final isothermal hold was at 125 ° C for three minutes. The scan rate was 4 deg/min. Because of the transient periods at the beginning and end of the scan, only data between 40 and 120 °C could be used for the heat capacity. An ice/water mixture was used as the coolant in the reservoir, and nitrogen was used as the purge gas.

The heat capacity of a sample was determined by combining the results form three different scans (O'Neill, 1966). At the beginning of a day's work a blank scan was made with an empty pan. This run accounted for how the pans coupled with the sample holders during scanning and was used as a baseline for the rest of the day. An empty pan was used in the reference cell of each run to cancel the thermal contribution of the pans. Next, a scan was made with a sapphire disk to calibrate the power axis. The standard run greatly improves the accuracy as described in Appendix A. Then, a sample run was made. Each sample was scanned two or three times. After the scans for a sample were completed, a second standard run was made. Then the next sample was run. Thus the sequence of runs was, blank, standard, sample run1, sample run2, standard, sample run1,.... Usually, three samples could be completed during the course of a day's work with this procedure.

The heat capacity was calculated by the scanning method according to the equation:

$$Cp = \frac{y}{y^s} \times \frac{m^s}{m} \times Cp^s$$

where Cp is the sample heat capacity, Cp^s is the heat capacity of sapphire, m is the sample mass, m^s is the mass of the sapphire standard, y is the displacement of the sample run from the blank run, and y^s is the displacement of the standard run from the

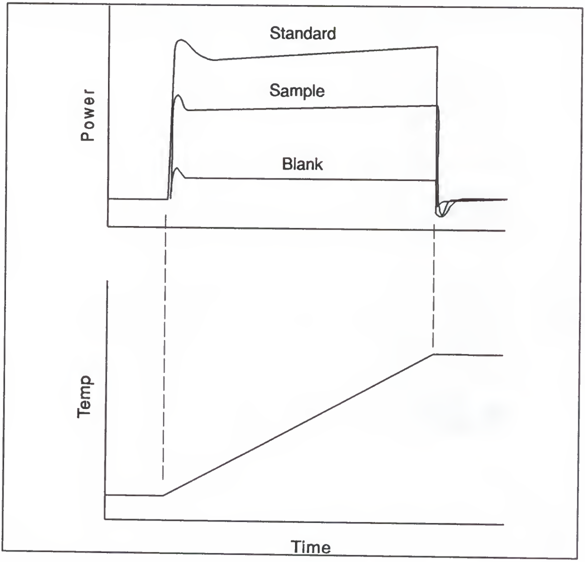

Figure 5. DSC scans used to determine the heat capacity of a sample

blank run (see Figure 5). Because different sample pans were used for the three scans, the results were corrected for the difference in pan masses. The data analysis procedure is described in detail in Appendix A.

Vapor-Liquid Equilibrium

We determined how the vapor pressure of water over black liquor changed with temperature and solids content by taking a series of pressure versus temperature readings at different solids contents for each liquor. To make these measurements conveniently, we constructed an apparatus which could be used for both the equilibrium measurements and concentrating the sample.

The apparatus has a five liter still pot which is larger than usual for two reasons. One, since we were concentrating samples we needed a large volume of initial material to have a reasonable amount of material left at the end. Two, black liquor foams considerably at lower concentrations and a large headspace is needed to control the foam.

The still pot has three parts: a glass sleeve, glass top and stainless steel bottom (see Figure 6). It hangs from a support frame by a clamp which holds the glass top and sleeve together. The top contains openings for the stirrer, condenser, pressure transducer, and platinum resistance thermometer. The bottom clamps to bottom of the glass sleeve and contains baffles and a drain port. It can be removed for cleaning without disturbing the rest of the apparatus.

An electric heating jacket slides over the stainless steel bottom and is connected to a variac to control the boil-up rate. A PID controller, pressure transducer, bleed valve, and vacuum pump make up the pressure control system. The controller operates the bleed valve which is connected between the vacuum pump and still to control the pressure in the still. A variable speed d.c. motor and a single turbine blade stirrer are

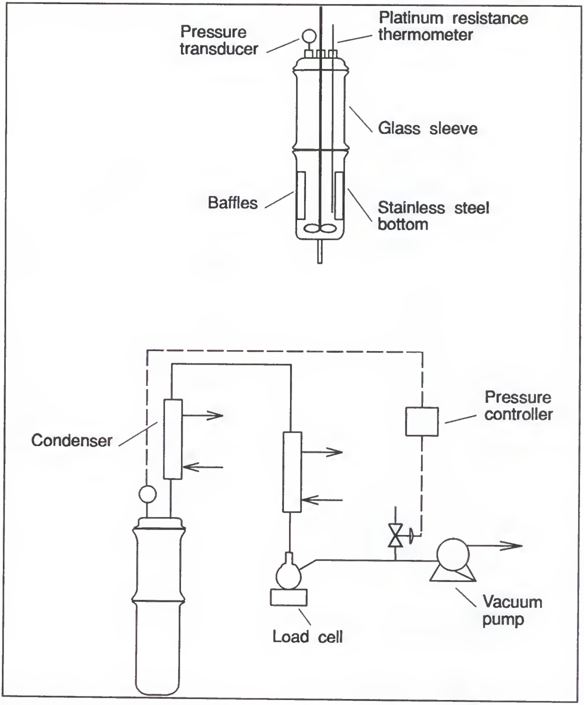

Figure 6. Schematic of vapor pressure apparatus

used for mixing. A stuffing box, filled with teflon packing, seals the stirrer shaft to prevent air from leaking into the system. The temperature of the liquor is measured with a platinum resistance thermometer. The output from the thermometer is connected to a linear bridge and read with a digital voltmeter.

A complete vapor pressure experiment consisted of running the apparatus under alternating cycles of constant reflux and evaporation. The operation was changed by turning the water on or off to the first condenser. While under constant reflux, a series of pressure versus temperature measurements were taken by first setting the pressure and then recording the temperature. When a complete data set was finished, the sample was concentrated to the next solids fraction and the procedure repeated. A load cell was used to record the amount of water evaporated off. The load cell was not accurate enough to determine the true solids content and, as a result, small samples were taken to determine the solids content. The samples concentrated in this work were used for the solution calorimetry work.

PRESENTATION AND ANALYSIS OF RESULTS

Data Presentation

Enthalpy-Concentration Charts

The charts for black liquor were constructed similarly to those for other aqueous systems (McCabe, 1935). Heat of dilution data were measured at one temperature over the concentration range of interest. A base isotherm for the chart was then determined from these data. The remaining isotherms were determined from heat capacity data measured over the concentration and temperature ranges of the chart.

Numerical values of enthalpy are not absolute quantities, but are the difference between the enthalpy in a given state and an arbitrary chosen reference state. The reference state of a mixture is established by choosing a reference state for each component in the mixture. The reference state is selected by specifying a convenient temperature, pressure, and composition. These conditions are arbitrary and may be different for the reference state of each component.

Because the charts are useful for binary systems only, black liquor was assumed to be a mixture of pure solids and water. For water, the same reference state as the steam tables, pure saturated water at 32 °F, was used. Thus, the steam tables can be used directly with the charts for the enthalpy of water vapor. An infinitely dilute solution reference state at 80 °C was used for the solids. This reference state was used instead of a pure solids reference state because enthalpy data are not needed up to 100% solids. The viscosity becomes too high to process the liquor, practically, above about

80% solids. Thus, there is an upper limit for the data which is defined by the viscosity. This boundary depends on temperature and, as a result, is not constant. In addition, enthalpy data below about 10% solids are not needed for the process conditions of the recovery cycle.

The enthalpy charts for four liquors, L1, L23, L31 and L51 are shown in Figures 7-10. Charts for the other liquors were not completed because of experimental errors. The charts allow the enthalpy of black liquor to be calculated over the range of 0-80% solids and 40-120 °C. The numerical values for the charts are given in Appendix A. Because the heat capacity measurements were made at different concentrations of solids from the heat of dilution measurements, a number of different interpolations of the experimental results were necessary to assemble the values for the charts. These interpolations, which are described in Appendix A, resulted in highly smoothed data.

Heat of Dilution Results

The results from a series of dilutions are shown plotted cumulatively on a scale of the total heat absorbed per gram of solids versus the concentration of solids in Figure 11. Since the heat of dilution of black liquor with water is exothermic, the ordinate scale is negative. This plot was made by assuming a value for the highest solids content and then adding the heats of dilution to it. The first dilution was made with the sample molded into a plug one time. The remaining dilutions were made two times and the results averaged.

When the results are connected by straight lines, the trend in the data of Figure 11 is easier to see. From 80% solids down to about 25% solids, the slope decreases gradually. Below 25% solids, the slope increases slowly before it increases rapidly for the final dilution. The dilutions between 55% and 25% had a precision of

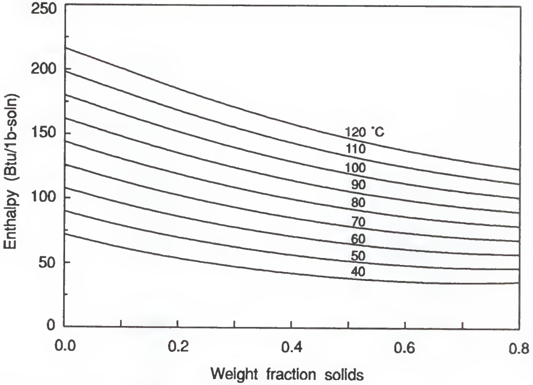

Figure 7. Enthalpy-concentration chart for liquor L1

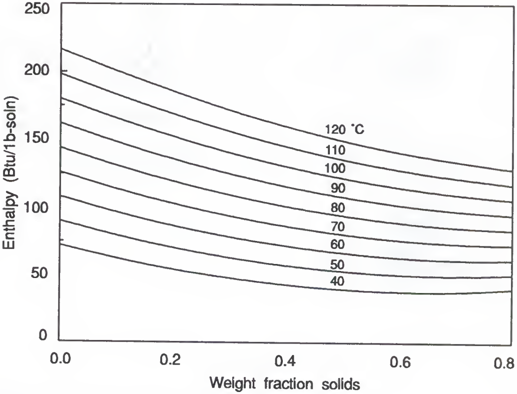

Figure 8. Enthalpy-concentration chart for liquor L23

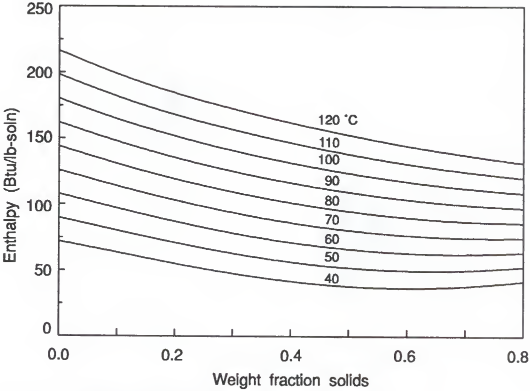

Figure 9. Enthalpy-concentration chart for Liquor L31

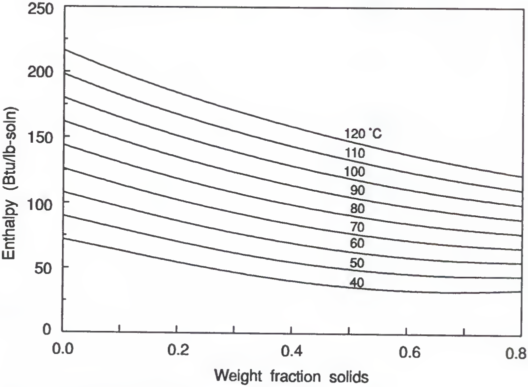

Figure 10. Enthalpy-concentration chart for liquor L51

about 1%. Below 25% the scatter increased to about 2%. The scatter was even higher, about 6%, for the last dilution from 5% to 1.667% solids. The increase in the slope and the decrease in precision of the dilutions at low solids contents suggested that a chemical reaction was taking place in addition to the mixing process. The association of lignin may have been the reaction taking place below 5% solids. Lignin is known to associate when the pH drops below about 12. The pH below 5% solids was calculated to be 12 to slightly above 12.

The purpose of plotting the data cumulatively was to determine the total heat of dilution to dilute black liquor to infinite dilution, Q^{∞}. At the final solids content of the data, 1.667% solids, the total heat of dilution did not intersect the ordinate scale. Because the data were of no practical interest below 5% solids, we extrapolated the data

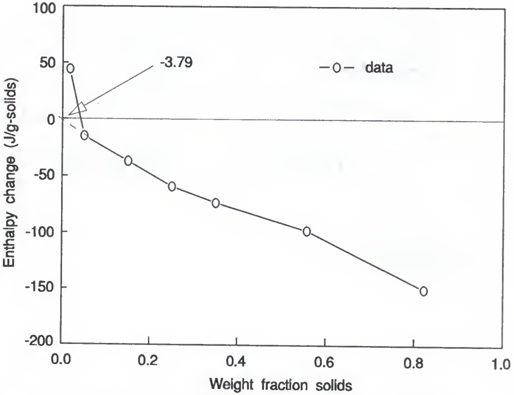

Figure 11. Plot of the total heat of dilution for a series of dilutions

to infinite dilution. A line, whose slope was determined from the dilution from 15% to 5% solids, was extrapolated to determine the y-intercept. For the data in Figure 11, the extrapolation gave a y-intercept of -3.79 J/g-solids. This value was used to adjust the scale to give a plot for the total heat of dilution to dilute a solution of a given solids content to infinite dilution.

The plots of Q^∞ for four liquors are compared in Figure 12. The lines in the figure are splines which are given only to show trends in the data. After the first two dilutions, each liquor was diluted in the same way. Although the results for all four liquors are qualitatively similar, they separate into two different groups. This is due to the results of the extrapolation used to complete the data. The slopes for all the liquors, including those for three additional liquors which are not shown, grouped around two separate mean values.

Once a plot for Q^∞ versus solids content was completed for a liquor, the enthalpy was calculated by the equation,

$$L = w_1 L_1 - w_2 Q^\infty \tag{4}$$

where Q^∞ is the heat absorbed to dilute a solution of enthalpy L to infinite dilution, L_1 is the enthalpy of pure water and w_1, w_2 are the weight fractions of water and solids, respectively (see Appendix A). Values of the enthalpy were determined by inserting values of Q^∞ and w_2 from the dilution experiments into eq. (4). These values gave the base isotherm at 80 °C for the charts.

A typical base isotherm along with the definition of the infinite dilution reference state is shown in Figure 13. Notice that the resulting isotherm is much smoother than the original heat of dilution data. The slope of the dashed line is equal to the slope of the curve at infinite dilution. It can be shown that the initial slope of the curve is equal to minus the enthalpy of pure water, which is -143.9 Btu/lb at 80 °C. When the line is

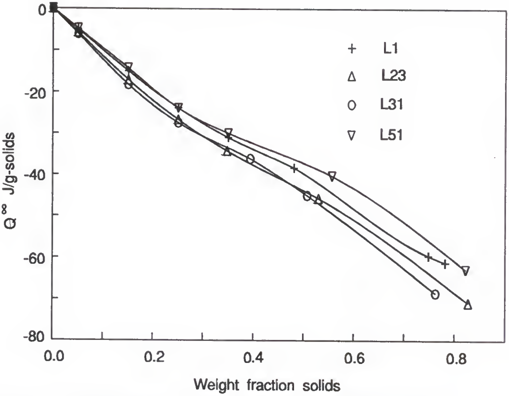

Figure 12. Heat absorbed to dilute black liquor to infinite dilution

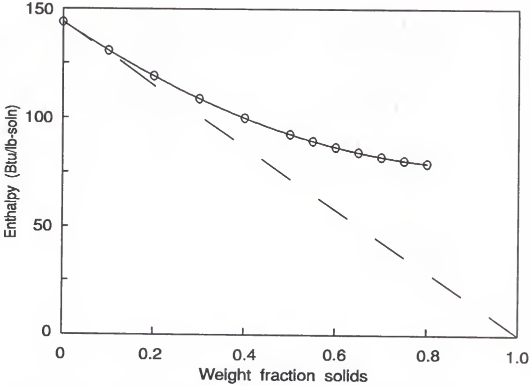

Figure 13. Base isotherm and definition of infinite dilution reference state

extrapolated from the value of the enthalpy for pure water to that for pure solids, it intersects the ordinate scale at a value of zero. The enthalpy is zero because the component, pure solids, is in its reference state. Thus, the infinitely dilute solution of solids in water is considered to be a pure component in the same state as a solution so dilute that no more heat would be absorbed upon further dilution. This, of course, is a hypothetical reference state for the solids. The base isotherm will be the only isotherm that will extrapolate to a value of zero; The remaining isotherms of the chart will extrapolate to finite values of the enthalpy. As the concentration of solids increases, the isotherm deviates more and more from the dashed line because the concentration is moving farther from the reference state.

Heat Capacity Results

The heat capacity at constant pressure, C_p, was needed to complete the remaining isotherms of the enthalpy concentration chart. It should be noted that we did not measure C_p by using DSC. We measured the heat capacity of the two-phase system, black liquor and water vapor at constant total volume. In general, this quantity is not equal to C_p. A flow calorimeter would be necessary to measure C_p directly. It is common practice, however, to measure the heat capacity of a liquid in equilibrium with a small amount of its vapor. The results can then be corrected to obtain C_p if volumetric data for liquid is available. The data necessary to make this correction for black liquor are not available. An estimate of the correction, which depends on the degree of filling, was calculated using water and was deemed small enough to ignore (see Appendix A). The correction, in general, will be negligible if the vapor pressure of the liquid and the amount of vapor space are small.

The experimental heat capacity data for each liquor are shown in Figures 14-17. Each curve in the figures is the results for a sample of a different concentration of solids.

The symbols are the actual data points and the lines are given only to show trends in the data. As shown, the heat capacity decreases with increasing solids content. The temperature dependence of the data appears to be linear due to the scale of the plots, but there is a slight curvature to the data. This curvature, as determined by least square fits of the data, was not constant and changed with solids content. At low solids, the data increased in a concave way with temperature. At high solids, the heat capacity generally reached a plateau with increasing temperature. As the solids content increases, the heat capacity increases more with temperature. At 10% solids, the heat capacity at 105 °C is about 3% higher than the value at 40 °C, and at 80% solids, it is about 5-6% higher.

For most of the samples in the figures, the results are the average of two temperature scans. Typically, the heat capacity versus temperature points of the second scan increased more uniformly with temperature than those of the first scan. The results from the first scan were not used when they appeared nonuniform. A nonuniform first scan was attributed to conditioning of the sample in the pan. This behavior was possible at all concentrations of solids. Above 50% solids, three scans were usually necessary because the first scan displayed a large dip in the results. This dip did not reappear in the second and third scans.

The difference between the average of the two scans and one of the scans was less than 0.5%. In those cases where the first scan appeared nonuniform this difference was about 1%. It was possible to fit the data with a polynomial of degree two to within 0.5%. Thus, the uncertainty of the raw data in terms of a temperature scan is less than 1%.

The heat capacity data for liquor L51 are shown plotted versus solids content in Figure 18 for two temperatures. The lines in the figure are from a multiple regression fit of all the data which included the additional points for the heat capacity of water and

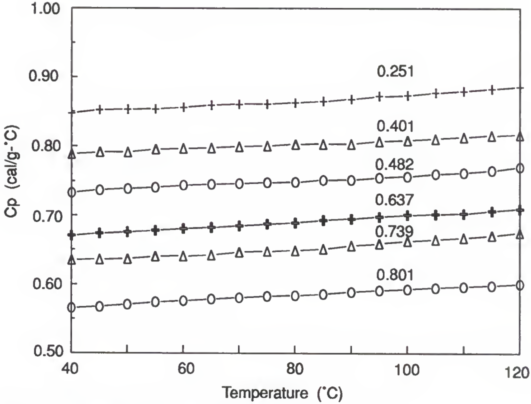

Figure 14. Heat capacity vs. temperature data for Liquor L1

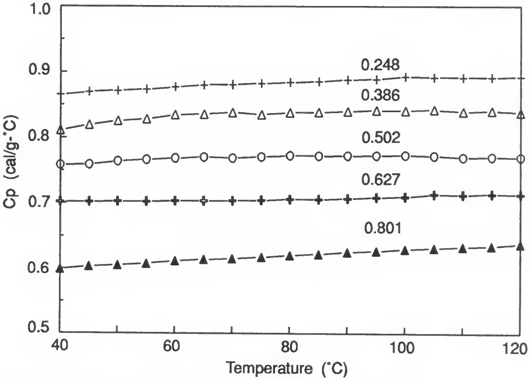

Figure 15. Heat capacity vs. temperature data for liquor L23

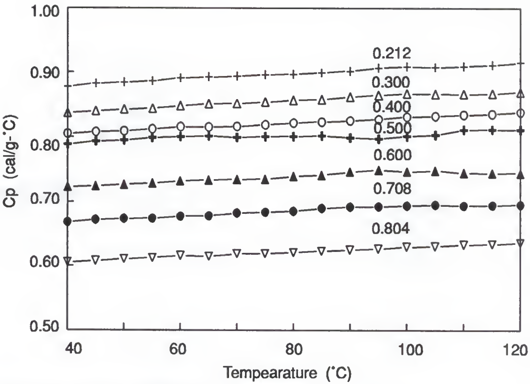

Figure 16. Heat capacity vs. temperature data for liquor L31

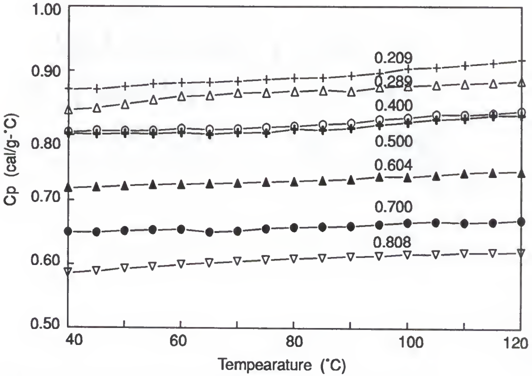

Figure 17. Heat capacity vs. temperature data for liquor L51

pure solids. The heat capacity for the solids was taken from Masse's results for a liquor from the same pulping conditions. The regression lines suggest that the heat capacity for liquor L51 does not change linearly with increasing solids content.

The scatter of the data about the regression lines for many of the data points is greater than 1%, which suggests that the experimental error is also greater than 1%. A set of tests was made, as a result, with three samples of the same solids content to estimate the experimental error (see Appendix A). The error from these tests was found to be 2%, which is believed to be a better estimate of the error. Thus, multiple DSC scans of a sample should not be considered as independent observations for a statistical analysis. Independent observations can only be obtained with different samples.

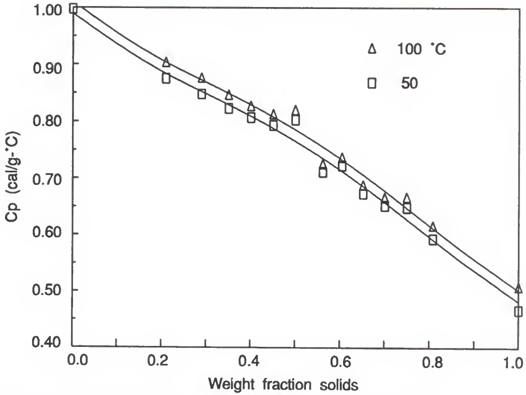

Figure 18. Heat capacity vs. solids content data for liquor L51

Notice that two points in Figure 18, at about 50% and 55% solids, differ by more than the 2% from the regression lines. Because the data were fitted by least-squares, these points probably contributed significantly to the shape of the regression curve. If these points had been considered outliers and not been used in the regression, the regression lines would have been much different. Notice also that the data between 40% and 75% solids do not change as much with temperature as the other points do. This behavior can also be seen in Figures 15-17 for liquors L23, L31, and L51.

In general, the results in the range of 40% to 75% solids were not consistent with those outside of this range. The heat capacity results in this range of concentrations may be influenced by the sample changing in some way. In black liquor, there is a phase inversion at about 50% solids to an organic continuous phase. It may be that DSC was measuring a heat effect associated with this transition.

Vapor Pressure Results

The pressure versus temperature behavior as function of solids content for liquor L51 is shown in Figure 19. This is typical of the results for all the liquors studied. Thus, the vapor pressure decreases as the solids content increases and its behavior with increasing temperature is similar at all solids contents. The symbols are the actual data points and the lines are from fits of the logarithm of the pressure versus 1/T with a polynomial of degree two. This is common way of treating vapor pressure data. It was possible to fit the data to about 1% with a polynomial of degree two.

The pressure versus temperature behavior for all the liquors is compared at three solids contents in Figures 20-22. A second interpolation was necessary to assemble the data for these graphs. The data were fitted to a polynomial in the solids content of degree two. The figures show that as the temperature increases the spread in the data increases. In Figure 20, the range of results at the final temperature is 34 mm Hg or

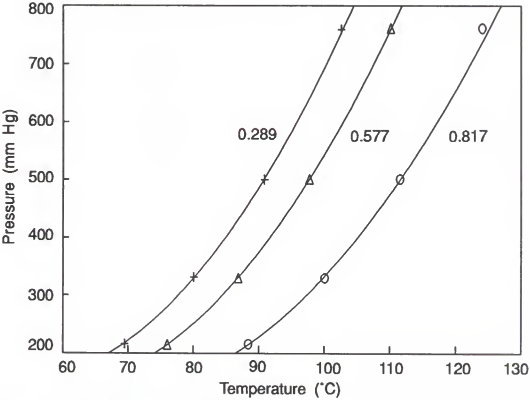

Figure 19. Vapor pressure versus temperature at three solids contents for liquor L51

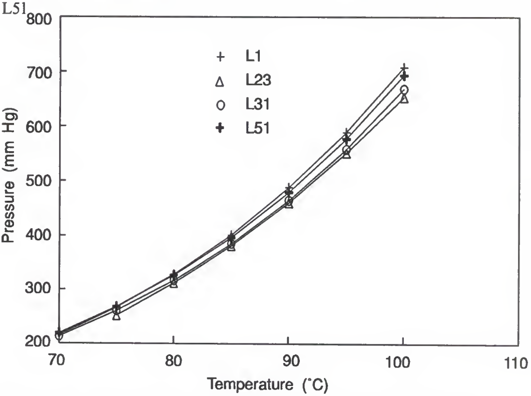

Figure 20. Vapor pressure versus temperature behavior at 30% solids

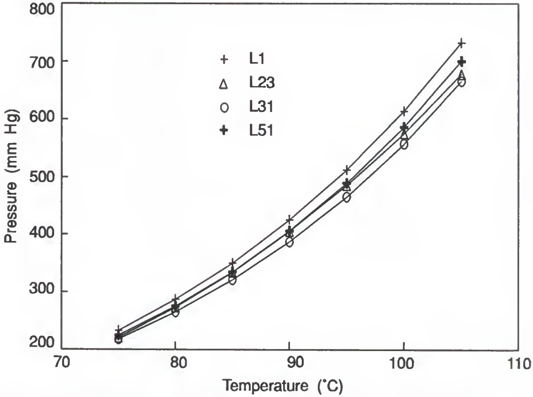

Figure 21. Vapor pressure versus temperature behavior at 50% solids

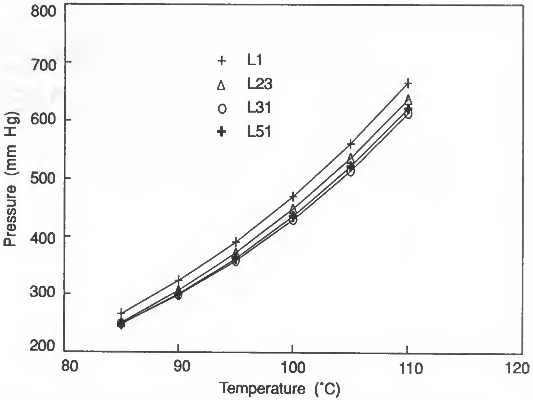

Figure 22. Vapor pressure versus temperature behavior at 70% solids

2.5% of the average for the range of results. In Figure 21, the range is 67 mm Hg or 5% of the average and in Figure 22 the range is 52 mm Hg or 4% of the average.

Notice that the P vs. T curves for three of the liquors in Figures 20-22 change sequence. Only the curve for liquor L1 is consistent with respect to the other three curves. The other curves overlap at low temperatures and change relative positions as the solids content increases. The vapor pressure is a colligative property at low concentrations of solids. If the vapor pressure is assumed, to a first approximation, to depend only the amount of solids at high solids contents, then the plots would not be expected to change position.

Calculated Vapor Pressures

The enthalpy chart data were used to generate vapor pressure data for comparison to the measured values. The vapor pressures were calculated for a given solids content from the knowledge of one vapor pressure using the equations in Appendix B. The pressure was calculated along the saturation curve by integrating the enthalpy data. The vapor pressure at atmospheric pressure of each vapor pressure data set was used as a reference condition for the calculations. This point was used because any error due to air leakage would be negligible at this condition.

The calculated vapor pressures are compared to the experimental values for liquor L51 in Table 5. Below the solids content of 53% solids, the calculated vapor pressures are less than the measured values. At 53% solids, there is good agreement with the data and above 53% solids, the calculated pressures are slightly greater than the measured values. If the enthalpy data are accurate and if this procedure can be used for black liquor, then the calculated results highlight the experimental errors in the measured values. In addition to the random experimental errors in the temperature and the pressure measurements, there are errors due to superheating of the liquor at high

Table 5. Comparison of calculated and experimental vapor pressures for L51

Solids %	Temp °C	Pexpt mm Hg	Pcalc mm Hg
20.94	68.45	216	207
	78.90	330	322
	89.69	500	494
	101.34	759	-
42.03	72.15	216	211
	82.59	330	326
	93.27	501	495
	105.10	761	-
53.08	75.79	216	213
	86.54	331	332
	97.36	501	501
	100.98	758	-
64.85	78.96	216	206
	90.16	331	325
	101.54	501	497
	113.72	761	-
78.17	86.14	216	219
	97.10	331	336
	108.43	501	507
	120.33	759	-
81.70	88.40	216	212
	100.07	330	332
	111.56	501	502
	124.04	761	-

solids contents and air leakage into the still at low pressures. Superheating raises the temperature above the equilibrium temperature and air leakage results in the pressure of water being less than the total pressure. If superheating can be ignored at low solids contents, then the calculated pressures show that there was some air leakage into the system. Air leakage would be possible if the teflon packing in the packing gland around the stirrer shaft became worn. Above 60% solids, superheating is likely and the calculated pressures would be greater than or equal to the measured values. The data in Table 5 follow this trend.

Data Analysis

The scale of the enthalpy charts depends on the type of procedure used to complete the heat of dilution data. We extrapolated the data to zero concentration of solids in an arbitrary way. The same procedure, however, was used for all the liquors. Note that some extrapolation will always be necessary to complete the data because the total heat of dilution cannot be measured experimentally. A different extrapolation would only shift the scale up or down and not affect the results above 5% solids. The results below 5% solids would change with a different extrapolation, but this range of concentration is not important for processing black liquor.

The data were extrapolated from a rather high concentration of solids because the pH may have dropped to value where lignin began associating. By extrapolating the data from 5% solids, changes in the configuration of the solids due to hydrogen bonding were ignored. Thus, the extrapolation approximates the heat evolved for changing the configuratin of the solids from their state at 5% solids to the infinitely dilute solution by dissolution only.

All the base isotherms are compared in Figure 23. The isotherms are all similar qualitatively deviating from each other only as the solids increases. This is a consequence of the infinite dilution reference state for the solids. All the isotherms must converge to the same point, the enthalpy of pure water, with the same slope. At 80% solids, the range between the smallest and largest isotherms is about 15 Btu/lb-soln.

The enthalpy concentration charts account for the enthalpy change for separating water from black liquor. This turns out to be a negligible contribution, however, as shown by the following example. Assume that black liquor is concentrated from 10% to 75% solids in a two step process. In the first step, the concentration of solids is changed from 10% to 75% solids by separating the required amount of water. In the second step, the water is evaporated. On a basis of 100 lbs of feed, the energy needed to separate water from black liquor is about 0.5% of the energy needed to evaporate the water.

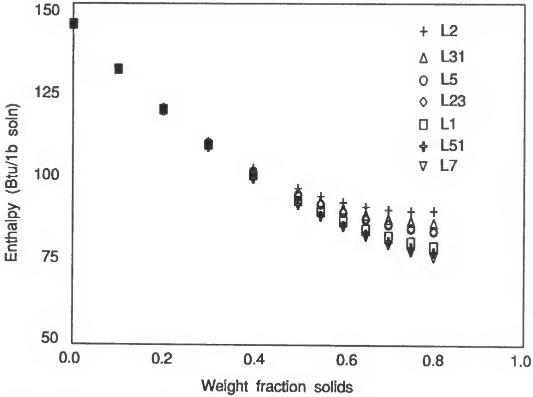

Figure 23. Comparison of base isotherms

The change in the heat capacity with increasing solids was not uniform for all liquors. Figures 24 and 25 show interpolated values of the heat capacity as a function of solids content. These values were used to develop the isotherms of the enthalpy concentration charts. As shown, the heat capacity for L1 changes linearly with solids content while that for L51 changes in a non-linear way. The behavior of the heat capacity with increasing solids content for L51 is qualitatively similar to that reported by Masse for a liquor with same pulping conditions. My results, however, have a greater dependence on temperature than the data reported by Masse. They are lower at 40 °C and higher at 105 °C than the results reported by Masse. The temperature dependence of my results is qualitatively similar to the results of Harvin and Brown. Harvin and Brown's data increase uniformly with temperature, however, compared to the compression of my data between 40 and 75% solids.

The fact that my results have a greater dependence on temperature than the results reported by Masse was of concern. Masse used DSC but with larger sample sizes, about 2 times as large, and a higher scan rate (10 deg/min). Also, Masse did not correct for the difference in pan masses. When the pan correction was important, it made more of a contribution at low temperatures. Masse, unfortunately, did not describe his sample preparation procedure in detail. He may have loaded the pans with pre-concentrated samples using a spatula. Note that it is not possible to load the pans uniformly with highly viscous samples using this procedure and that the results obtained from DSC are sensitive to the sample preparation. He also may have used too high of a scan rate for the sample size he used. If so, the sample would not have been at a uniform temperature during scanning.

If Masse's results are correct, then the results obtained by DSC may depend on the sample size. No detailed study of the effect of scan rate and sample size was made in this work. Different sample sizes were tried before the final sample preparation

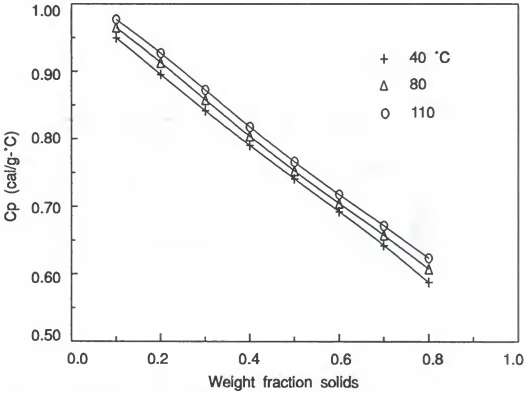

Figure 24. Fitted values of the heat capacity for liquor L1

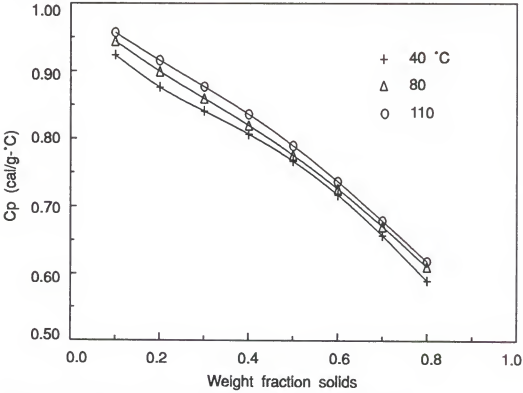

Figure 25. Fitted values of the heat capacity for liquor L51

procedure was decided upon. When the sample size was less than 20 mg, the change in heat capacity with increasing temperature was greater than the results reported earlier. Larger sample sizes, for example 70 mg, produced results which varied less with increasing temperature and which were generally inconsistent.

A boiling point elevation plot is a more useful way of presenting vapor pressure data when there is only one volatile component. Because the boiling point of water is subtracted from the experimental data, the plot is also a more critical test of the data than a P vs T plot. The experimental error is on the same order of magnitude as the ordinate scale in this type of plot. Figure 26 shows a BPE plot for liquor L51 as a function of pressure. This plot is typical of all the results. The boiling point elevation plot should start at a value of zero. The curves for 250 and 450 mm Hg would not

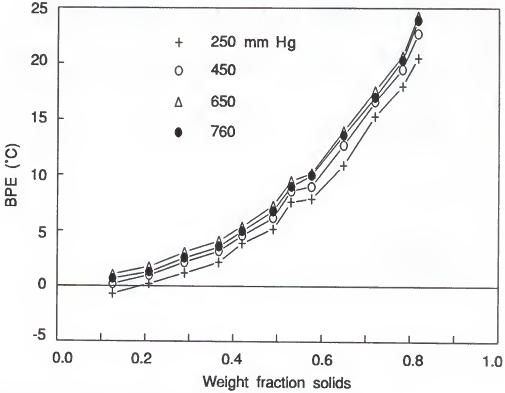

Figure 26. Boiling point elevation plot for liquor L51

extrapolate to zero which suggests these curves may be in error by a constant. Both superheating of the liquor and leakage of air into the still will cause errors in the BPE results. Superheating will raise the BPE and air leakage will cause the BPE to be low.

At atmospheric pressure, the results should not be affected by air leakage and, as a result, can be compared more confidently. Estimates of the BPE from the raw data as a function solids content are given in Table 6. No attempt was made to fit the BPE curves because of the scatter in the points. Also shown in Table 6 are typical values from the literature. Thus, the results for the four liquors are very close and are in the same range as the best-fit data given by Clay and Grace (1984).

The calculated and measured values of the vapor pressure are shown in Figure 27 for the vapor pressure data of liquor L51. The symbols are interpolations of the measured vapor pressures and the second curve for each solids content is the calculated vapor pressure using the measured value at atmospheric pressure as a reference. Although the calculated and measured vapor pressures do not agree, the calculated values do predict the correct trend of the measured values. The agreement at 70% solids is better, probably, because of offsetting errors in the measured data. Thus, vapor pressures can be calculated from the enthalpy data which are at least as accurate as the measured values.

Table 6. Comparison of BPE estimates with literature values

Liquor	50%	60%	70%	80%
Estimates of Boiling Point Elevations from Experimental Data				
L1	6.5	11	17	-
L23	6	10	13	-
L31	9	13	16	-
L51	8	12	16	23
Literature Values				
Clay	6.5	11	17	24.5
Szymonski & Grace	10	14	20	30

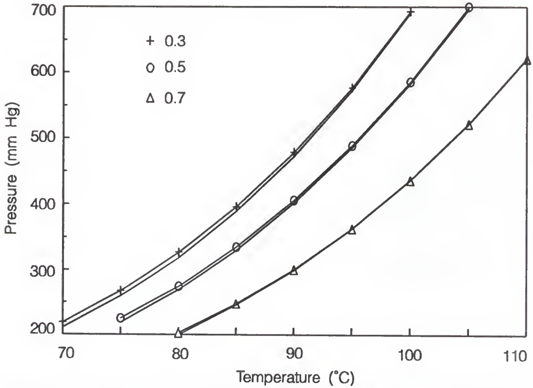

Figure 27. Comparison of calculated and measured vapor pressures for liquor L51

CONCLUSIONS AND RECOMMENDATIONS

The objective of this investigation was to develop a consistent set of enthalpy and vapor pressure data for Kraft black liquor. To accomplish this, the heat of dilution and heat capacity were measured for different liquors and the results used to develop enthalpy concentration charts. Vapor pressures were measured for the same set of liquors and then compared to the values calculated from the enthalpy data. Because black liquor can be a highly variable material, liquors from laboratory cooks of slash pine were used instead of mill liquors. The liquors were taken from a wide range of pulping conditions so that a wide range of behavior might be expected.

Enthalpy concentration charts which cover the range of 0-80% solids and 40-120 °C were determined for four liquors. The charts incorporate the enthalpy change for separating water from black liquor, which has been ignored in the past. This heat effect, however, is negligible when compared to the heat of vaporization of water and, as a result, does not contribute significantly to the energy balance around the evaporators. No significant difference was found among the charts for the four liquors studied. Thus, black liquor can be treated as a pseudo-binary mixture of solids and water and, as a result, all black liquors can be considered to be the same in terms of the enthalpy.

The heat of dilution of water with black liquor is a measure of how strongly water interacts with the components of black liquor. The larger the heat of dilution the more strongly water interacts with the other components. The heats of dilution which we measured were small exothermic quantities. Because of the many components in black liquor, the measured heats of dilution were the sum of many possible interactions. The net interaction did not result in a large heat effect.

There are many components in black liquor that could interact strongly with water. For example, the enthalpy change for separating water from a solution of sodium hydroxide, over the concentration range of sodium hydroxide in black liquor, is about four times greater than the enthalpy change for separating water from black liquor. Thus, the presence of the organics reduces the interaction between water and the inorganics.

Since heat of dilution of water with black liquor is small and moderated by the organics to some extent, the results reported here are probably representative of all liquors. Note that only one type of liquor, a softwood liquor from slash pine, was used in this work.

We found that the heat capacity does not change linearly with increasing solids content above 30% solids. This result agrees qualitatively with earlier results reported by Masse. This behavior, however, was not uniform for all the liquors studied. The results reported here have a larger temperature dependence than the results reported by Masse. This dependence on temperature agrees qualitatively with results reported by Harvin and Brown. The small difference in the heat capacities among the liquors studied was largely canceled when the data were integrated for the enthalpy charts.

There is still some uncertainty in the results obtained from differential scanning calorimetry, particularly in the concentration range from 40% to 75% solids. The results in this concentration range were not consistent with those outside of this concentration range. The results may be influenced by the phase inversion that occurs in black liquor in this concentration range. Or, the scan rate (4 deg/min) may have been too high. The only way to determine the accuracy of the results reported here would be to measure the heat capacity at much lower scan rates, for example, at less than 1 deg/min. This would involve a considerable amount of experimental effort, but the results should allow the concentration and temperature dependence of the heat capacity to be determined more accurately. Since the results reported here suggest that the heat capacity does not vary widely from liquor to liquor, this could be done for one liquor only.

Boiling point elevation plots of the vapor pressure data revealed experimental errors that were greater than initially thought. As a result, only estimates of the BPE as a function of solids content could be made. There was little difference in the BPE values among the four liquors studied and with those reported in the literature. A small change in BPE with pressure was observed, but the results were not precise enough to determine the change of BPE with pressure accurately.

The vapor pressures calculated from the enthalpy data predicted the correct trend of the measured vapor pressures and are thermodynamically consistent with the enthalpy data. The calculated values, however, tended to deviate from the measured values at low pressures. Whether the cause of this deviation was due to the measured data or the calculation procedure could not determined. To calculate the vapor pressure from the enthalpy data, requires accurate vapor pressure data at one temperature. The vapor pressure, as a result, should be measured carefully at one condition to provide a reliable reference condition. Once a reliable vapor pressure is available, the vapor pressures should calculated again to determine how well they agree with the measured values.

APPENDIX A
DETAILED DISCUSSION OF THE ENTHALPY WORK

Derivation of the Working Equation for the Enthalpy Scale

The heat absorbed when pure water is added to a solution of black liquor is given by

$$\Delta H = H_{final} - H_{initial} \tag{5}$$

where H_{final} is the enthalpy after mixing and $H_{initial}$ is the enthalpy of pure water and the initial solution. If enough water is added to change the composition by a finite amount, then ΔH is called an integral heat of dilution.

Suppose black liquor is assumed to be a mixture of two components, water and pure solids. The equation,

$$H = m_1 \bar{H}_1 + m_2 \bar{H}_2 \tag{6}$$

where $\bar{H}_i$ is the partial specific enthalpy of i and m_i is the mass of i, relates the enthalpy of a binary mixture to the composition of the mixture. The partial specific enthalpies are assigned to the components in a mixture according to a systematic procedure, but the components do not actually have these properties (Smith and Van Ness, 1975).

Substituting eq. (6) into eq. (5) gives the enthalpy change,

$$\Delta H = m_1' \bar{H}_1' + m_2 \bar{H}_2' - m_1 \bar{H}_1 - m_2 \bar{H}_2 - (m_1' - m_1) H_1 \tag{7}$$

for adding $(m_1' - m_1)$ grams of water to a solution containing m_2 grams of black liquor solids and m_1 grams of water. The enthalpies in eq. (7) are absolute quantities which are not known. The calorimetric measurements, as a result, do not lead to numerical values of the enthalpy directly. If an arbitrary reference state is chosen, then the difference between the enthalpy in any state and the reference state can be tabulated.

Let $\bar{H}_i^\circ$ be the partial specific enthalpy of component i in the reference state for i. Adding and subtracting the $\bar{H}_i^\circ$'s to eq. (7) gives

$$\begin{aligned}\Delta H &= m_1'(\bar{H}_1' - \bar{H}_1^\circ) + m_2(\bar{H}_2' - \bar{H}_2^\circ) - m_1(\bar{H}_1 - \bar{H}_1^\circ) - m_2(\bar{H}_2 - \bar{H}_2^\circ) \\ &\qquad - (m_1' - m_1)(H_1 - \bar{H}_1^\circ) \\ &= m_1'\bar{L}_1' + m_2\bar{L}_2' - m_1\bar{L}_1 - m_2\bar{L}_2 - (m_1' - m_1)L_1\end{aligned} \tag{8}$$

where $\bar{L}_i$ is the relative partial specific enthalpy of component i. The relative enthalpy, L, is used as a reminder that the enthalpy is a relative quantity.

Since water is the solvent, choose the pure component reference state for it. For the solids, choose the infinitely dilute solution of solids in water. The reference state enthalpies in eq. (8) become H_1° for water and $\bar{H}_2^{\circ\infty}$ for the solids. Then, as the amount of solids goes to zero, the relative partial specific enthalpies become

$$\begin{aligned}\bar{L}_1 &\rightarrow L_1 = H_1 - H_1^\circ \\ \bar{L}_2' &\rightarrow \bar{L}_2'^{\infty} = \bar{H}_2^{\infty} - \bar{H}_2^{\circ\infty} \quad .\end{aligned} \tag{9}$$

The infinite dilution reference state for the solute is a hypothetical one. The solute is considered to be a pure component in the same state as in a solution so dilute that no measurable heat effect is obtained on further dilution.

If the amount of water added is so large that no more heat is absorbed upon further dilution, then eq. (8) reduces to

$$Q^{\infty} = m_1 L_1 + m_2 \bar{L}_2^{/\infty} - L \qquad (10)$$

where Q^{∞} is the total heat absorbed for a constant weight of solute. If the temperature of the dilution experiment is selected as the temperature of the reference state, then $\bar{L}_2^{/\infty}$ is zero and eq. (10) reduces to

$$Q^{\infty} = m_1 L_1 - L\ . \qquad (11)$$

Thus, the enthalpy of a solution is determined from the total heat absorbed when the solution is diluted to infinite dilution and the enthalpy of water. In practice, this dilution is not carried out in one step but in a series of successive steps so that the enthalpy along the isotherm can be determined.

Construction of the Chart

The base isotherm for the charts was determined from eq. (11) and the plot of Q^{∞} versus solids content. Rearranging eq. (11) gives

$$L = (1 - w_2)L_1 - w_2 Q^{\infty} \qquad (12)$$

which allows L to be determined from values of the weight fraction of solids, w_2, and Q^{∞}. The enthalpy was calculated at the weight fractions corresponding to the dilution experiments. The value of the enthalpy for pure water was taken from the steam tables. The enthalpy data were then fitted to a second order polynomial in the weight fraction of solids.

The remaining isotherms of the chart were determined from the heat capacity data. The heat capacity data were measured at different solids contents from those of charts and, as a result, had to be interpolated to get values at the solids contents for the charts.

First, each heat capacity data set was fitted to a second-order polynomial in temperature. Then, for each temperature, the smoothed values were fitted to a fourth-order polynomial in the weight fraction of solids. For this fit, values of the heat capacity for water and the pure solids were added to the data. This was done so that the first derivative near the ends of the data would give proper values. The derivative of data was needed to calculate the vapor pressure in a subsequent step (see Appendix B). Values of the enthalpy at 80 ° C and the heat capacity were interpolated from the resulting polynomials for the enthalpy tables. The values of the heat capacity for the enthalpy chart were then fitted to second-order polynomial in temperature. This polynomial was then integrated from 80 ° C to each temperature of chart and the results added to enthalpy of the base isotherm.

Enthalpy Tables

The numerical values of the enthalpy that correspond to Figures 7-11 are given in the following tables.

Table 7. Enthalpy for liquor L1

Enthalpy (Btu/1b)								
Temp	Solids Content							
°C	0.10	0.20	0.30	0.40	0.50	0.60	0.70	0.80
40	61.8	53.9	47.5	42.5	38.7	36.3	35.3	36.1
45	70.3	61.9	55.1	49.6	45.4	42.5	41.1	41.4
50	78.9	70.0	62.7	56.7	52.1	48.8	46.9	46.7
55	87.5	78.1	70.3	63.9	58.8	55.0	52.7	52.0
60	96.1	86.2	77.9	71.0	65.5	61.3	58.6	57.4
65	104.7	94.4	85.6	78.2	72.2	67.6	64.4	62.8
70	113.4	102.6	93.3	85.4	78.9	73.9	70.3	68.2
75	122.0	110.7	100.9	92.6	85.7	80.2	76.2	73.6
80	130.7	119.0	108.7	99.8	92.5	86.5	82.1	79.1
85	139.4	127.2	116.4	107.1	99.2	92.9	88.0	84.6
90	148.1	135.4	124.1	114.3	106.0	99.3	94.0	90.1
95	156.8	143.7	131.9	121.6	112.9	105.6	99.9	95.6
100	165.6	152.0	139.7	128.9	119.7	112.0	105.9	101.2
105	174.4	160.2	147.5	136.2	126.5	118.5	111.9	106.7
110	183.1	168.6	155.4	143.6	133.4	124.9	117.9	112.3
115	191.9	176.9	163.2	150.9	140.3	131.3	124.0	117.9
120	200.8	185.2	171.1	158.3	147.2	137.8	130.0	123.6

Table 8. Enthalpy for liquor L31

Enthalpy (Btu/1b)								
Temp	Solids Content							
°C	0.10	0.20	0.30	0.40	0.50	0.60	0.70	0.80
40	63.7	55.2	47.7	41.8	38.0	36.8	38.1	41.8
45	72.0	63.2	55.3	49.1	45.1	43.4	44.2	47.3
50	80.3	71.1	63.0	56.5	52.1	50.0	50.2	52.7
55	88.7	79.1	70.6	63.9	59.2	56.6	56.3	58.2
60	97.1	87.1	78.3	71.3	66.3	63.3	62.5	63.7
65	105.5	95.1	86.1	78.8	73.4	70.0	68.6	69.2
70	113.9	103.1	93.8	86.2	80.5	76.7	74.8	74.7
75	1122.3	111.1	101.6	93.7	87.7	83.4	81.0	80.3
80	130.8	119.2	109.4	101.2	94.8	90.1	87.1	85.9
85	139.2	127.3	117.2	108.7	102.0	96.9	93.4	91.5
90	147.7	135.4	125.0	116.3	109.2	103.6	99.6	97.1
95	156.2	143.5	132.9	123.8	116.4	110.4	105.8	102.8
100	164.7	151.7	140.7	131.4	123.6	117.1	112.1	108.4
105	173.2	159.8	148.6	139.0	130.8	123.9	118.4	114.1
110	181.8	168.0	156.6	146.6	138.0	130.6	124.7	119.8
115	190.3	176.2	164.5	154.2	145.3	137.4	131.0	125.5
120	198.9	184.4	172.5	161.8	152.5	144.2	137.3	131.2

Table 9. Enthalpy for liquor L51

Enthalpy (Btu/1b)								
Temp	Solids Content							
°C	0.10	0.20	0.30	0.40	0.50	0.60	0.70	0.80
40	63.4	54.7	46.9	40.5	36.0	33.4	32.8	34.1
45	71.7	62.6	54.5	47.8	42.9	39.8	38.7	39.4
50	80.0	70.5	62.1	55.1	49.8	46.3	44.6	44.7
55	88.4	78.5	69.7	62.4	56.7	52.7	50.6	50.1
60	96.8	86.4	77.3	69.7	63.6	59.2	56.5	55.5
65	105.2	94.4	85.0	77.0	70.5	65.7	62.5	60.9
70	113.7	102.5	92.7	84.3	77.5	72.2	68.5	66.4
75	1122.1	110.5	100.3	91.6	84.4	78.7	74.5	71.9
80	130.6	118.6	108.1	99.0	91.4	85.2	80.6	77.3
85	139.1	126.7	115.8	106.4	98.4	91.8	86.6	82.9
90	147.7	134.9	123.6	113.8	105.3	98.3	92.6	88.4
95	156.2	143.0	131.4	121.2	112.4	104.9	98.7	93.9
100	164.8	151.2	139.2	128.6	119.4	111.4	104.8	99.5
105	173.3	159.4	147.0	136.0	126.4	118.0	110.9	105.0
110	181.9	167.6	154.8	143.5	133.5	124.6	117.0	110.6
115	190.5	175.9	162.7	151.0	140.5	131.2	123.1	116.2
120	199.1	184.1	170.6	158.5	147.6	137.8	129.2	121.8

Heat Capacity Measurements

I followed many of the suggestions given by Callanan and Sullivan (1986) for obtaining accurate thermodynamic data using DSC. Because DSC is a comparative technique, the instrument was calibrated under the same conditions as those used for the experiments. The melting point of indium (156.6 °C) was used to calibrate the temperature axis. Once a melting point scan was made, the calibration was done automatically by the system software. It was possible to calibrate the temperature axis to within 0.01 °C of the melting point standard. The power axis was calibrated with a sapphire standard as shown below.

Importance of the Standard Run with Sapphire

The power supplied to a sample during a DSC scan depends on the sample's mass and heat capacity. If we think of the output as it would be recorded on a chart recorder, then the heat flow into the sample is given by

$$K \times y = m \times C_p \times \frac{dT}{dt} \tag{13}$$

where K is the ordinate calibration factor in cal./inch-sec., y is the ordinate deflection in inches, m is the sample mass in grams, C_p is the heat capacity in cal/gram-°C, dT/dt is the program rate in °C/min.

In principle, the heat capacity can be determined from eq. (13) once the sample and blank runs have been completed. The accuracy will depend on how well the power axis has been calibrated with melting point standards. The power axis, however, cannot be calibrated as well as the temperature axis. The accuracy can be improved significantly by making a third run with a standard such as sapphire.

Writing a similar equation for the standard run we get

$$K \times y^s = m^s \times C_p{}^s \times \frac{dT}{dt} \tag{14}$$

where *s* denotes the standard run.

Dividing eq. (13) by eq. (14) and rearranging gives the heat capacity for the sample,

$$C_p = \frac{y}{y^s} \times \frac{m^s}{m} \times C_p{}^s \tag{15}$$

in terms of the heat capacity of sapphire. Thus, the standard run eliminates the ordinate calibration factor and program heating rate from the heat capacity calculation. The heat capacity of sapphire has been determined to five significant figures by Ginnings and Furukawa (1953).

Two standard runs were made for each sample run, one before and one after. The two standard runs account for instrument drift, contamination of the sample holders, and differences in position of the pans from run to run during the course of a days work. The average value for the two standard runs was used in eq. (15) to determine the sample heat capacity.

Stainless Steel Pans

The pans are designed to be used with liquid samples and can withstand a pressure of 350 psi. Their large volume (0.075 ml) made them easier to load but results with these pans will, in general, be poorer than with aluminum pans because of their larger mass, lower thermoconductivity, and poorer coupling with the sample holders. In addition, the aluminum covers that fit over the sample holders could not be used because the pans were too tall. Using the covers would have resulted in more consistent results. (It may have been possible to use the aluminum covers by bowing them out slightly so they did not touch the pans, but this was not tried.)

The same empty, standard, and reference pans were always used. A different sample pan was used for each sample. The mass of different pans varied by as much as 5 mg which was significant enough to correct for. The blank run will not cancel the effect of the pans if there is a difference in pan mass between the blank run and sample runs. A pan heavier than the blank pan, for example, would result in an increase in the observed heat capacity. To correct for this, the correction, eq. (16),

$$F = (m_p - m_b)\cdot C_{pan}\cdot S \tag{16}$$

where F is the amount of correction, m_p is the mass of the specimen pan, m_b is the blank pan mass, C_{pan} is the heat capacity of the pan material, and S is the scan rate, should be subtracted from each standard and sample run. Thus, if the difference in pan masses is greater than one, a correction is subtracted from each data point. When this correction was tried, however, it gave results which were consistently too low. The reason for this was not determined.

It was decided that the correction should be made by adjusting the blank run by the ratio of the specimen pan to the blank pan mass. A corrected blank run was obtained by, eq. (17),

$$y^{bc} = ((m_p - m_b)/m_b + 1)y^{bo} \tag{17}$$

where y^{bc} is the corrected blank run and y^{bo} is the observed blank run, before subtracting from the standard and sample runs. The correction to the heat capacity for the pan masses was about 1% and had more of an effect at low temperatures than at high temperatures. The mass of the O-rings varied also but was not corrected for.

Sample Size

Depending on the amount of sample used in the stainless steel pans there can be a relatively large vapor space above the sample. Because it is desirable to use a small sample size, I was concerned that the results may be in error due to the water that evaporates from the liquid into the vapor space. As a result, I calculated the correction to the measured heat capacity for water.

Rowlinson and Swinton (1982) derive the necessary equations for relating C_σ, the heat capacity of a saturated liquid and Cp to the experimental heat capacity of a two-phase system. The heat capacity of a two-phase system is composed of three parts, the saturation heat capacity of the liquid, that of the vapor, and the heat required to evaporate δn moles of liquid. That is,

$$C = n^l C_\sigma^l + n^g C_\sigma^g - T\gamma_\sigma(n^l v^l \alpha_\sigma^l + n^g v^g \alpha_\sigma^g) \tag{18}$$

where l,g denote the saturated liquid and gas respectively, n is the number of moles, v is the molar volume, γ_σ is the thermal pressure coefficient along the saturation curve, and α_σ is the coefficient of thermal expansion along the saturation curve. It is possible to simplify eq. (18) by eliminating C_σ^g to give

$$C = n(C_\sigma^l - T\gamma_\sigma^l \alpha_\sigma^l) + n^g T\Delta v(\partial^2 P/\partial T^2)_\sigma \tag{19}$$

where n is the total number of moles and $\Delta v = (v^g - v^l)$. It is also possible to simplify eq. (19) in terms of Cp. That is,

$$C = n[Cp^l - T\gamma_\sigma v^l(2\alpha_p^l - \beta_T^l \gamma_\sigma)] + n^g T\Delta v(\partial^2 P/\partial T^2)_\sigma \tag{20}$$

where β_T is the coefficient of isothermal compressibility.

Using eq. (19), I calculated the difference between the measured heat capacity and heat capacity of the saturated liquid for different amounts of water. If 50% of the pan (about 37 mg) was filled with water, then the difference at 80 °C was one-half percent. At 100 °C, the difference was about one percent.

For black liquor, if the sample size was less than about 20 mg, the heat capacity curve became concave upward and increased rapidly above 90 °C. It was found that this behavior could be changed by loading the pans with more sample. The heat capacity curve then changed to a convex shape and generally reached a plateau above 90 °C. We used about the minimum sample necessary to change the heat capacity curve to give those shown in the results.

Method of Data Analysis

Because the DSC data were digitally recorded, the data files from each scan contained a series of power versus temperature points. A computer program was written to subtract the blank run from the standard and sample runs for the values in eq. (15). The first step of the analysis was to align the starting and ending isotherms of the blank run with those of the standard and sample runs. The starting and ending isotherms were different for each scan. When the beginning isotherms of the blank and sample or standard runs were aligned, therefore, the ending isotherms did not match. This was corrected for by sloping the blank run until the ending isotherms matched.

Figure 28 illustrates how the blank scan was sloped. The pivot point and slope points correspond to the last data point of isothermal hold and temperature ramp, respectively. Each point between the pivot and slope points was rotated through an angle theta about the pivot point to give a corrected scan. To calculate the angle theta, the difference between the ending isotherms was added to the slope point to give the new slope point. The angle theta, then, was determined by the difference of the angles of the

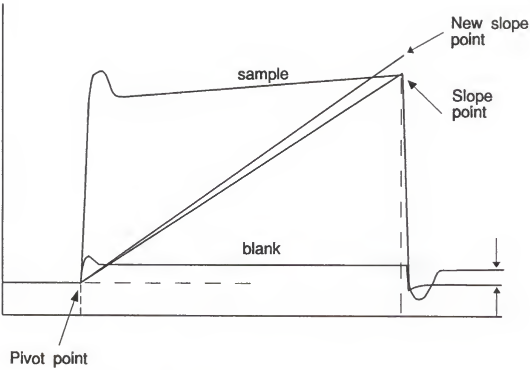

Figure 28. Method for aligning ending isotherms.

original and new slope points formed with the pivot point. Before the blank run was sloped, the correction for the pan masses, eq. (17) was applied.

After the sloping procedure, the time points of the blank scan no longer corresponded to the original points. An interpolation was done to determine the power levels that correspond to the original time points. The blank run was then subtracted from the sample or standard runs.

The sloping procedure turned out to be significant. The difference between the ending isotherms was different for each run and was greater for the sample runs. Sloping had the most affect on the points near the end of the scan.

Uncertainty Analysis

The minimum uncertainty and the controlling error in the Cp measurement was determined from the following analysis. The equation for heat capacity was differentiated with respect to each of the measurable variables to give,

$$\Delta C_p = \sqrt{(\frac{\partial C_p}{\partial y})^2(\Delta y)^2 + (\frac{\partial C_p}{\partial y^s})^2(\Delta y^s)^2 + (\frac{\partial C_p}{\partial m})^2(\Delta m)^2 + (\frac{\partial C_p}{\partial m^s})^2(\Delta m^s)^2}$$

where

$$\frac{\partial C_p}{\partial y} = \frac{m^s}{m}\cdot\frac{C_p^s}{y^s} \qquad \frac{\partial C_p}{\partial m} = \frac{y}{y^s}\cdot C_p^s\left(-\frac{m^s}{m^2}\right)$$

$$\frac{\partial C_p}{\partial y^s} = \frac{m^s}{m}\left(-\frac{1}{y^s}\right)^2 y\cdot C_p^s \qquad \frac{\partial C_p}{\partial m^s} = \frac{y}{y^s}\cdot\frac{C_p^s}{m}$$

The quantities, Δy and Δm are the uncertainties in the power level and mass, respectively. The uncertainty in the mass is the random error in weighing the samples and Δy is the random error in the power level. The above analysis assumes the errors in the power level and mass are random and that the variables are independent of each other. The power level and mass are correlated, however. As the mass increases the power level increases proportionately. Thus, it is not strictly correct to differentiate them to find the error. But, it is possible to run several experiments holding the composition and mass approximately constant to estimate the uncertainty in the power level.

Typical values for use in the above equation were taken from a group of tests with approximately the same mass and composition. From the example calculation shown in Figure 29, the following can be noted:

1. The minimum uncertainty in the Cp measurement by DSC is about 1%.
2. The controlling error is due to the term for the standard run.
3. The power level for the standard run, y^s should be greater than one and greater than the power level for the sample run.
4. Errors in the mass do not contribute to the error significantly.

The uncertainty was also estimated by making several duplicate tests. Table 10 shows the results for three different samples of approximately the same solids content which were scanned two times. The results were treated as three samples of two observations each. The mean and variance were calculated for each sample and then combined to calculate the overall mean and standard deviation. The mean and standard deviation are shown in Table 11. Thus, the uncertainty, as estimated by the standard deviation, is about 2% and greater than the estimate of 1% from above. This is probably a more realistic estimate of the experimental error.

The uncertainty from the duplicate tests was greater due to drift of the instrument, differences in position of the pans on the sample holder and thermal contact between the pans and sample holder.

Values for sample calculation:

Solids content = 0.5076 T = 40 °C

$m^s = 26.396$ mg

$m = 32.972$ mg

$y^s = 1.41827$ mW

$y = 6.83559$ mW

$\Delta y^s = 0.012$ mW

$\Delta y = 0.012$ mW

$Cp^s = 0.19256$ cal/g-C

$Cp = 0.7409$ cal/g-C

Substitiuting the above into the partial differentials and evaluating them gives:

$$\frac{\partial C_p}{\partial y} = 0.10869 \qquad \frac{\partial C_p}{\partial m} = 0.02253$$

$$\frac{\partial C_p}{\partial y^s} = 0.52386 \qquad \frac{\partial C_p}{\partial m^s} = 0.02815$$

$$\Delta Cp = [(0.10869)^2(0.012)^2 + (0.52386)^2(0.012)^2 + (0.02253)^2(0.01)^2 + (0.02815)^2(.01)^2]^{1/2}$$

$$\begin{aligned} \Delta Cp &= [1.70115 \times 10^{-6} + 3.9517 \times 10^{-5} + 5.0760 \times 10^{-8} + 7.92423 \times 10^{-8}]^{1/2} \\ &= 0.0064 \\ &= 0.7409 \pm 0.0064 \end{aligned}$$

Figure 29. Sample calculation for uncertainty in Cp measurement by DSC

Table 10. Heat capacity results for three samples of the same solids content

Temp. C	#1, 0.5076		#2, 0.5053		#3, 0.5078	
	1A	1B	2A	2B	3A	3B
40	.7409	.7450	.7451	.7480	.7299	.7306
45	.7468	.7473	.7485	.7508	.7320	.7333
50	.7474	.7477	.7494	.7499	.7344	.7335
55	.7524	.7504	.7538	.7546	.7379	.7361
60	.7550	.7542	.7558	.7657	.7410	.7375
65	.7567	.7554	.7557	.7569	.7406	.7380
70	.7567	.7556	.7558	.7579	.7424	.7390
75	.7599	.7586	.7572	.7600	.7413	.7398
80	.7613	.7602	.7573	.7617	.7432	.7421
85	.7610	.7627	.7577	.7653	.7454	.7479
90	.7613	.7642	.7564	.7652	.7428	.7451
95	.7671	.7673	.7658	.7680	.7460	.7481
100	.7628	.7658	.7673	.7698	.7484	.7505
105	.7652	.7672	.7714	.7712	.7508	.7540
110	.7666	.7675	.7696	.7726	.7522	.7539
115	.7648	.7686	.7699	.7742	.7523	.7554
120	.7660	.7702	.7713	.7744	.7516	.7565

Table 11. Mean and standard deviation of samples for uncertainty analysis

Temperature °C	Mean Cp	Standard Deviation
40	.7399	.0140
45	.7431	.0150
50	.7437	.0139
55	.7476	.0150
60	.7500	.0153
65	.7505	.0159
70	.7512	.0150
75	.7528	.0174
80	.7543	.0165
85	.7567	.0141
90	.7558	.0169
95	.7604	.0189
100	.7608	.0164
105	.7633	.0160
110	.7637	.0154
115	.7642	.0153
120	.7650	.0160

APPENDIX B
DETAILED DISCUSSION OF THE VAPOR PRESSURE WORK

Relationship Between the Enthalpy and Vapor Pressure

If the vapor pressure is replaced with the fugacity, the vapor phase does not have to be assumed ideal initially. The change in the fugacity of water with temperature at constant pressure and composition is given by

$$\frac{\partial \ln f_w}{\partial T} = \frac{(H_w^* - \bar{H}_w)}{RT^2} \tag{24}$$

where H_w^* is the enthalpy of water in a state of zero pressure and $\bar{H}_w$ is the partial molar enthalpy of water. The difference, $(H_w^* - \bar{H}_w)$ is the enthalpy change for expanding water into a vacuum and is called the ideal heat of vaporization of water. Subtracting a similar equation to eq. (24) for a mixture with a different composition from eq. (24) gives

$$\frac{\partial \ln f_w}{\partial T} - \frac{\partial \ln f'_w}{\partial T} = \frac{\bar{H}'_w - \bar{H}_w}{RT^2} \tag{25}$$

or, upon rearranging,

$$\frac{\partial \ln (f_w / f'_w)}{\partial (1/T)} = \frac{\bar{H}_w - \bar{H}'_w}{R}\ . \tag{26}$$

Since the composition of the mixture was not specified, and therefore is arbitrary, let the initial composition be that of pure water. Thus, eq. (26) becomes,

$$\frac{\partial \ln(f_w/f_{wp})}{\partial(1/T)} = \frac{\bar{H}_w - H_w}{R} \tag{27}$$

where f_{wp} and H_w are the fugacity and enthalpy of pure water, respectively. The enthalpy terms in eq. (27) are absolute quantities, but as discussed in Appendix A, the enthalpy can only be calculated above an arbitrary reference state. Thus, the enthalpies should be replaced with the relative enthalpies. Making this notation change and integrating eq. (27) from a reference temperature, T' to a temperature T gives

$$\ln\frac{f_1}{f_{1p}} = \ln\frac{f_1'}{f_{1p}'} + \frac{M_1}{R}\int_{T'}^{T}(\bar{L}_1 - L_1)d(\frac{1}{T}) \tag{28}$$

where M_1 is the molecular weight of water. It is assumed that the fugacity of water over the solution is known at the temperature T'. Thus, the fugacity can be calculated from the enthalpy data for the mixture and pure water.

The pressure can be calculated from the fugacity by the equation,

$$\frac{\partial \ln f}{\partial P} = \frac{V}{RT} \tag{29}$$

where V is molar volume of water. Subtracting the quantity,

$$\frac{\partial \ln P}{\partial P} = \frac{1}{P} \tag{30}$$

from both sides of eq. (29) gives

$$\frac{\partial \ln f/P}{\partial P} = \frac{V}{RT} - \frac{1}{P} \quad . \tag{31}$$

Integrating eq. (31) from a pressure, P^* to a pressure P gives

$$\ln f/P - \ln f^*/P = \int_{P^*}^{P}(\frac{V}{RT} - \frac{1}{P})dP \quad . \tag{32}$$

If we let $P^* \rightarrow 0$ in eq. (32), then $f^* \rightarrow P$ by definition. Thus, eq. (32) becomes

$$\ln f/P = \int_0^P \left(\frac{V}{RT} - \frac{1}{P}\right) dP \tag{33}$$

which relates the fugacity to vapor pressure. Equation (33) can be written in terms of the compressibility factor, $z = PV/RT$, to give

$$\ln f/P = \int_0^P (z-1)\frac{dP}{P} \quad . \tag{34}$$

At low pressures, the quantity, $(z - 1)$ is equal to BP/RT where B is the second virial coefficient (Smith and Van Ness, 1975). Substituting this expression into eq. (34) gives the equation,

$$\ln f/P = \frac{BP}{RT} \tag{35}$$

which allows the vapor pressure to be determined easily from the fugacity.

Calculation of Vapor Pressures from Enthalpy Data

The fugacity along the saturation curve for a given solids content was calculated from eq. (28) and the following equations. First, values for the relative partial specific enthalpy as a function of temperature were calculated form the enthalpy data for the base isotherm and heat capacity data by

$$\bar{L}_1(T) = \bar{L}_1(T_0) + \int_{T_0}^{T} \bar{C}_{p_1}\, dT \tag{36}$$

where $\bar{C}_{pl}$ is the partial specific heat capacity of water. As part of the data analysis for the enthalpy chart, the enthalpy data for the base isotherm and heat capacity data were fitted to polynomials in the weight fraction of solids. From these polynomials, $\bar{L}_1$ and $\bar{C}_{pl}$ were determined by the equations:

$$\bar{L}_1 = L - w_2 \frac{dL}{dw_2} \tag{37}$$

$$\bar{C}_{p1} = C_p - w_2 \frac{dC_p}{dw_2} \quad . \tag{38}$$

Applying equations (37) and (38) to the enthalpy and heat capacity data resulted in new polynomials in the weight fraction of the solids. Equation (37) was evaluated at the temperature of base isotherm (80 °C), and eq. (38) was evaluated at a number of different temperatures for the solids contents of the vapor pressure data. These values were then fitted to a polynomial in temperature of degree two which was then integrated for use in eq. (38) to give the partial specific enthalpy of water. Values of the enthalpy of water were used to calculate the quantity, $(\bar{L}_1 - L_1)$ which was then fitted to a polynomial in $(1/T)$ of degree two.

For each vapor pressure data set, one data point was chosen as a reference condition. The fugacity at the reference condition was calculated from the vapor pressure by eq. (35). The fugacity of pure water was calculated at the reference temperature by eq. (35) also. The integral of eq. (28) was evaluated from the reference temperature to each additional point of the data set and then added to the ratio of fugacities at the reference condition. The pressure was calculated from the fugacity by using eq. (35). Values for the second virial coefficient were taken from O'Connell and Prausnitz (1970).

REFERENCE LIST

Adams, T.L., and Frederick, J., Kraft Recovery Boiler Physical and Chemical Processes. New York: The American Paper Institute, 1988.

Callanan, J.E., and Sullivan, S.A., "Development of Standard Operating Procedures for Differential Scanning Calorimeters." Rev. Sci. Instrum. 57(10), 2584 (1986).

Clay, D.T., and Grace, T.M., "Measurements of High-Solids Black Liquor Boiling Point Rise." Tappi J. 67(2), 92 (1984).

Fricke, A.L., Physical Properties of Kraft Black Liquor: Final Report-Phase I. DOE report no. DOE/CE/40606-T1 (DE84006996). Washington, D.C., 1983.

Fricke, A.L., Physical Properties of Kraft Black Liquor: Summary Report-Phases I and II. DOE report no. DOE/CE/40606-T5 (DE88002991). Washington, D.C., 1987.

Fricke, A.L., A Comprehensive Program to Develop Correlations for the Physical Properties of Kraft Black Liquors. DOE report no. DOE/CE/40740-T4 (DE89016404). Washington, D.C., 1989.

Ginnings, D.C., and Furukawa, G.T., "Heat Capacity Standards for the Range 14 to 1200 °K." J. Am. Chem. Soc. 75, 522 (1953).

Harvin, R.L., and Brown, W.F., "Specific Heat of Sulphate Black Liquor." Tappi 36(6), 270 (1953).

Jelinek, S.F., "Black Liquor Heat of Mixing and Enthalpy from Heat Capacity Data." Tappi J. 69(8), 114 (1986).

Masse, M.A., Thermal Analyses of Kraft Black Liquor, M.S. Thesis, University of Maine, (1984).

Masse, M.A., Kiran, E., and Fricke, A.L., "A Thermodynamic Model of the Heat Capacity of Compositionally Complex Multicomponent Polymer Solutions: Kraft Black Liquor." Chem. Eng. Comm. 50, 81 (1987).

McCabe, W.L., "The Enthalpy-Concentration Chart. A Useful Device for Chemical Engineering Calculations." Trans. AIChE, 31, 129 (1935).

O'Connell, J.P. and Prausnitz, J.M., "Thermodynamic and Transport Properties of Water Vapor at Low Densities." Ind. Eng. Chem. Fund. 9, 579 (1970).

O'Neill, M.J., "Measurement of Specific Heat Functions by Differential Scanning Calorimetry." Anal. Chem. 38(10), 1331 (1966).

Rowlinson, J.S., and Swinton, F.L., Liquids and Liquid Mixtures. 3rd ed. London: Butterworths, 1982.

Sjorstrom, E., Wood Chemistry: Fundamentals and Applications. New York: Academic Press, 1981.

Smith, J.M., and Van Ness, H.C., Introduction to Chemical Engineering Thermodynamics. 3rd ed. New York: McGraw-Hill, 1975.

Szymonski, K.A., and Grace, T.M., "A Method of Measuring the Water Vapor Pressure of Black Liquor." Tappi J. 68(2), 87 (1985).

BIOGRAPHICAL SKETCH

I graduated from the University of Michigan and then worked in industry for two years. Then, I came to the Department of Chemical Engineering at the University of Florida not knowing what I know now. I wish I had known then what I know now.

I certify that I have read this study and that in my opinion it conforms to acceptable standards of scholarly presentation and is fully adequate, in scope and quality, as a dissertation for the degree of Doctor of Philosophy.

Arthur L. Fricke

Arthur L. Fricke, Chair
Professor of Chemical Engineering

I certify that I have read this study and that in my opinion it conforms to acceptable standards of scholarly presentation and is fully adequate, in scope and quality, as a dissertation for the degree of Doctor of Philosophy.

Balaban

Murat O. Balaban
Associate Professor of Food Science and
Human Nutrition

I certify that I have read this study and that in my opinion it conforms to acceptable standards of scholarly presentation and is fully adequate, in scope and quality, as a dissertation for the degree of Doctor of Philosophy.

Charles L Beatty

Charles L. Beatty
Professor of Materials Science

I certify that I have read this study and that in my opinion it conforms to acceptable standards of scholarly presentation and is fully adequate, in scope and quality, as a dissertation for the degree of Doctor of Philosophy.

Gar B. Hoflund

Gar B. Hoflund
Professor of Chemical Engineering

I certify that I have read this study and that in my opinion it conforms to acceptable standards of scholarly presentation and is fully adequate, in scope and quality, as a dissertation for the degree of Doctor of Philosophy.

Gerald B Westermann-Clark

Gerald B. Westermann-Clark
Associate Professor of Chemical Engineering

This dissertation was submitted to the Graduate Faculty of the College of Engineering and to the Graduate School and was accepted as partial fulfillment of the requirements for the degree of Doctor of Philosophy.

May, 1992

Winfred M. Phillips
Dean, College of Engineering

Madelyn M. Lockhart
Dean, Graduate School